UV wind estimation using sequential images from VEX VMC

Takeshi Horinouchi, Shinichi Ikegawa

(Hokkaido Univ)

Paper: Ikegawa & Horinouchi (2015) *Icarus*, submitted: **IH15**

Data

- VEX VMC (Venus Monitoring Camera) V 2.0
  - 365 nm (UV). 512x512 px
  - per 20~30 min. (higher freq. than in earlier missions)

Purpose

- To improve the cross-correlation method using multiple images

Preprocess

- Select images to use
  - by exposure time (<30ms) and by eyes (do not use low-quality images)
  - Resolution at sub-spacecraft point (SSP) 20 - 40 km = SSP latitude 66S - 47S
  - Thin out images if time interval < 10 min
- Optical distortion correction (Kouyama et al 2013) and limb fitting（Ogohara et al 2012） by using the **Akatsuki L3 software**
- Brightness correction by Belton et al (1990) (used satellite zenith angle > 75°& solar zenith angle > 80°)
- Interpolate onto lon-lat grid: 0.125°

Possible wrong match in the cross-correlation (CC) method

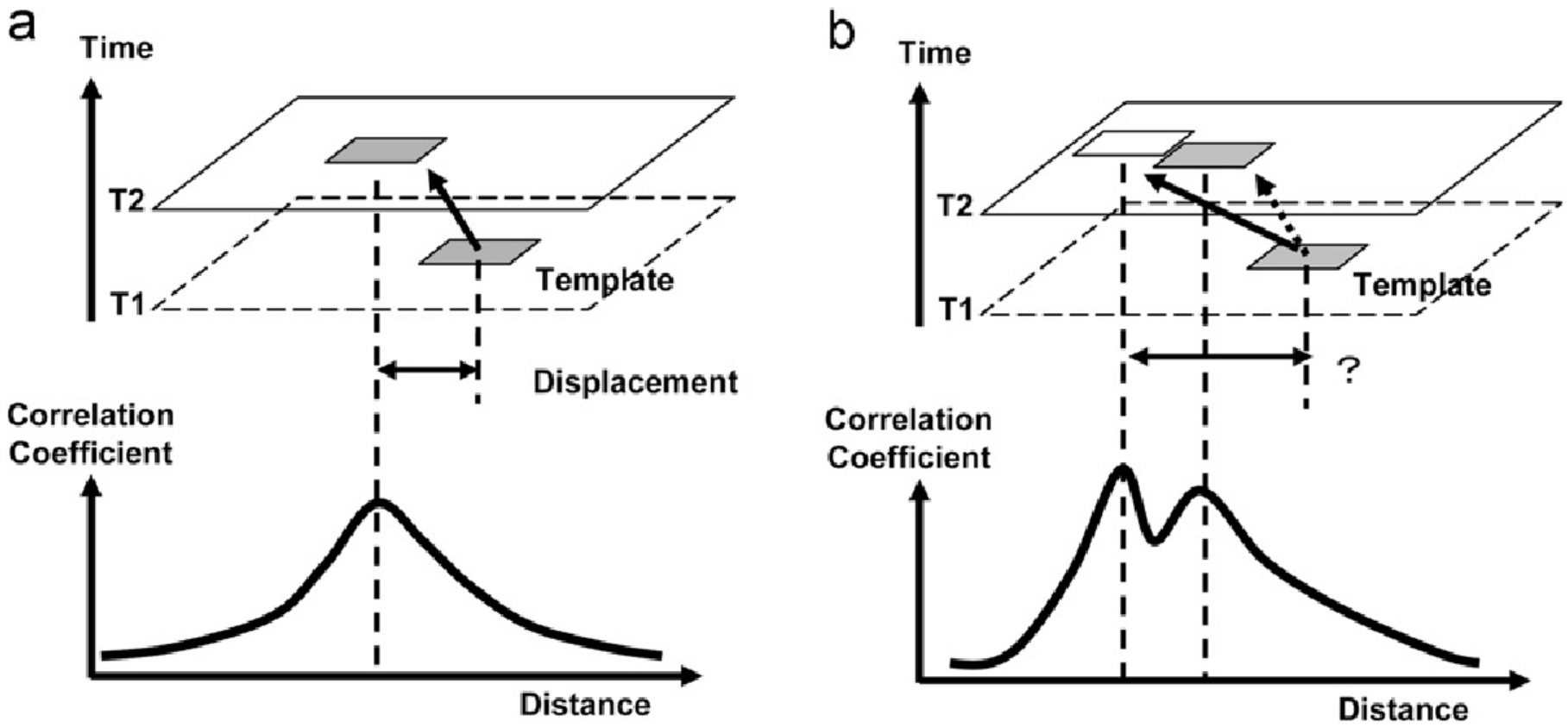

From Kouyama et al. (2012)

Example of the CC surfaces with multiple peaks（VMC orbit #246, Δt = 3h20m）

Template size 6°x6°

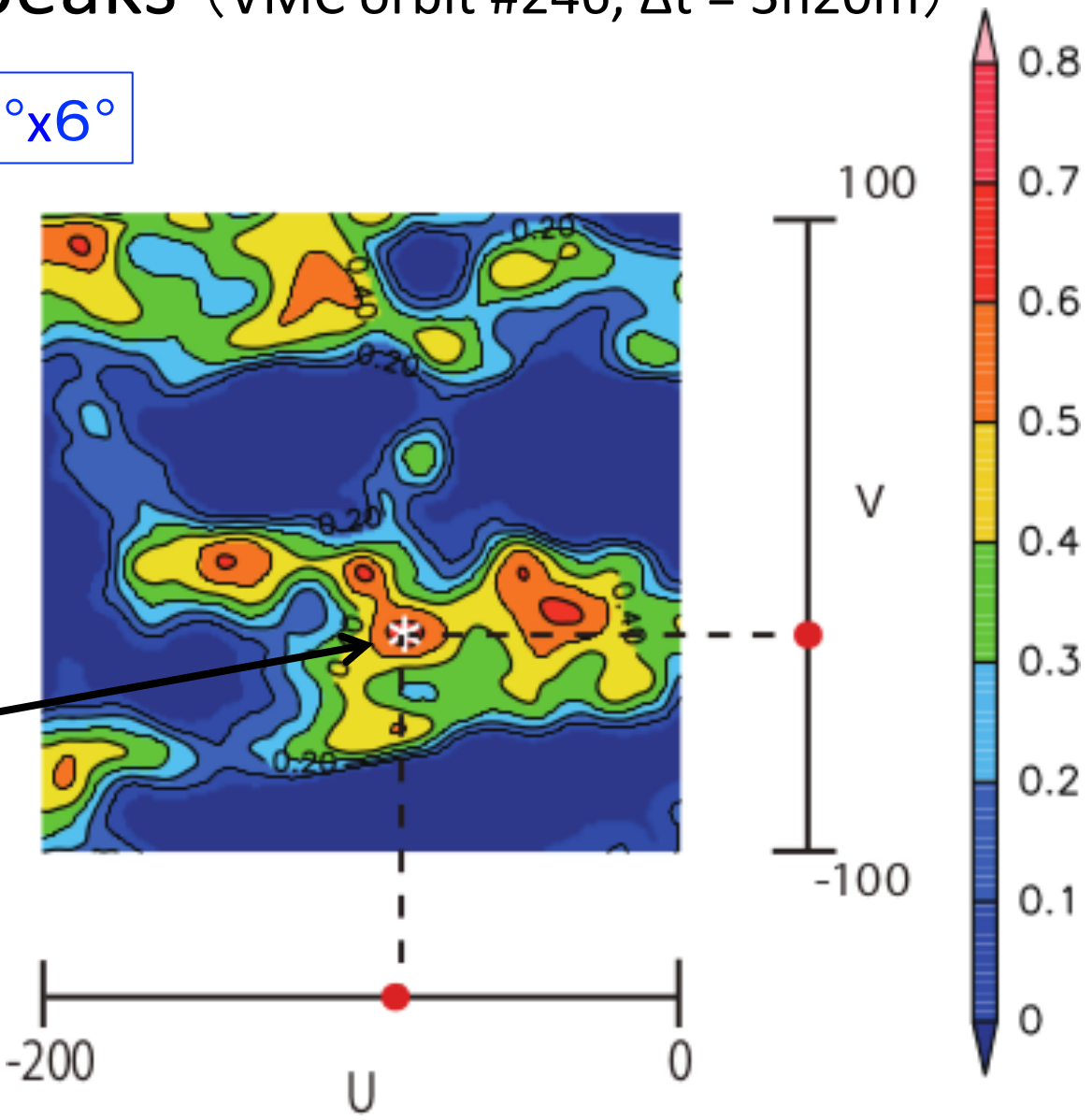

Maximum:
wrong match

Original VMC images (Titov et al 2012)

Raw

Corrected; available via ftp

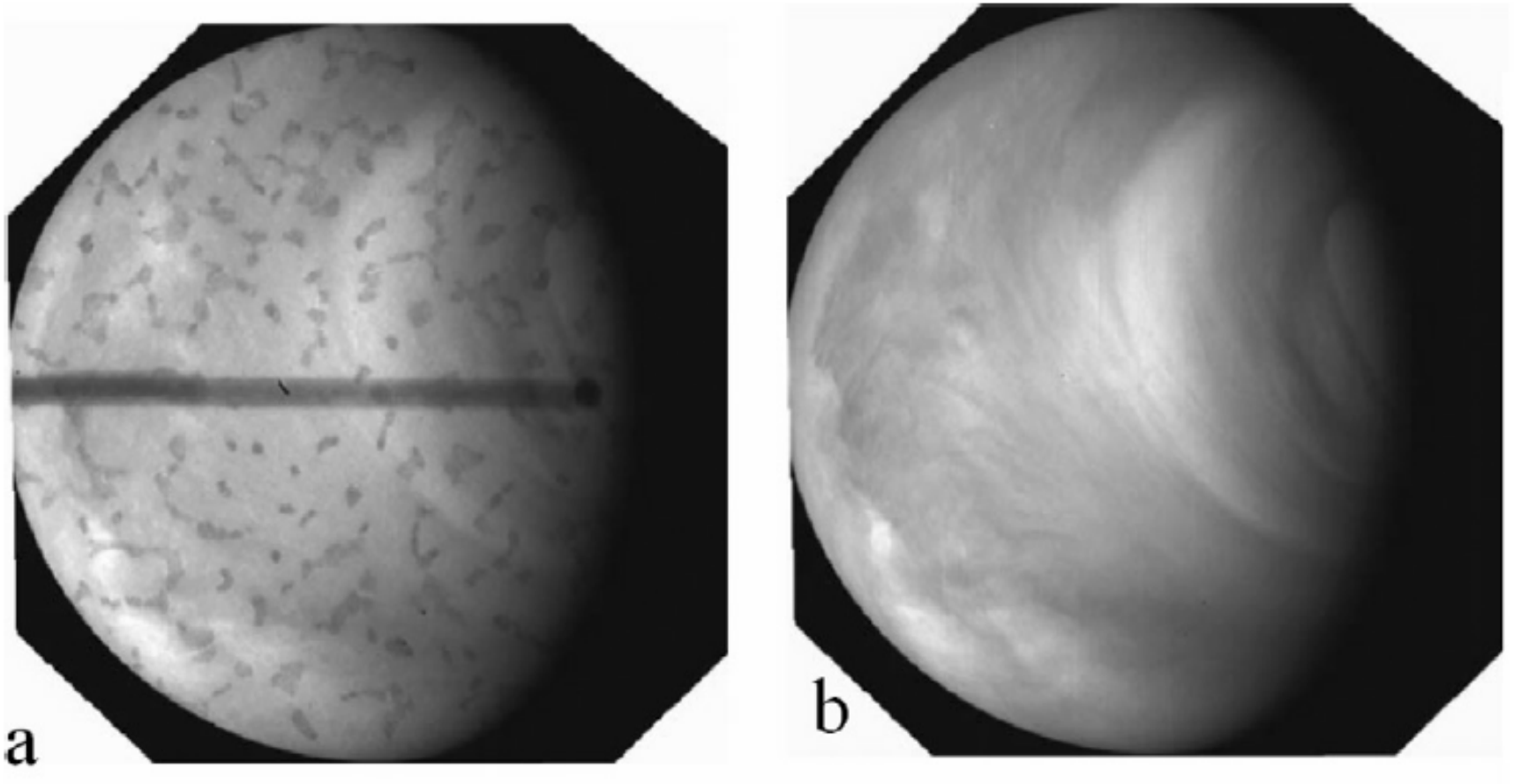

Fig. 3. Examples of the VMC data products in the UV channel: raw image (a), calibrated and flat fielded image (b), ...

VMC 2.0 data

- Corrected, but noise still remains (sometimes only partially & faintly, sometimes largely & significantly)
- Noise patterns often have similar scales to signal scales → sometimes makes tracking difficult

⇒ We would need a noise tolerant method

How to use multiple images

- Superpose the CC surfaces between 2 images for all combinations with $\Delta t >= \Delta t_{min}$ (=40 min in this study)
  - **Point:** superpose with respect to velocity (u,v)

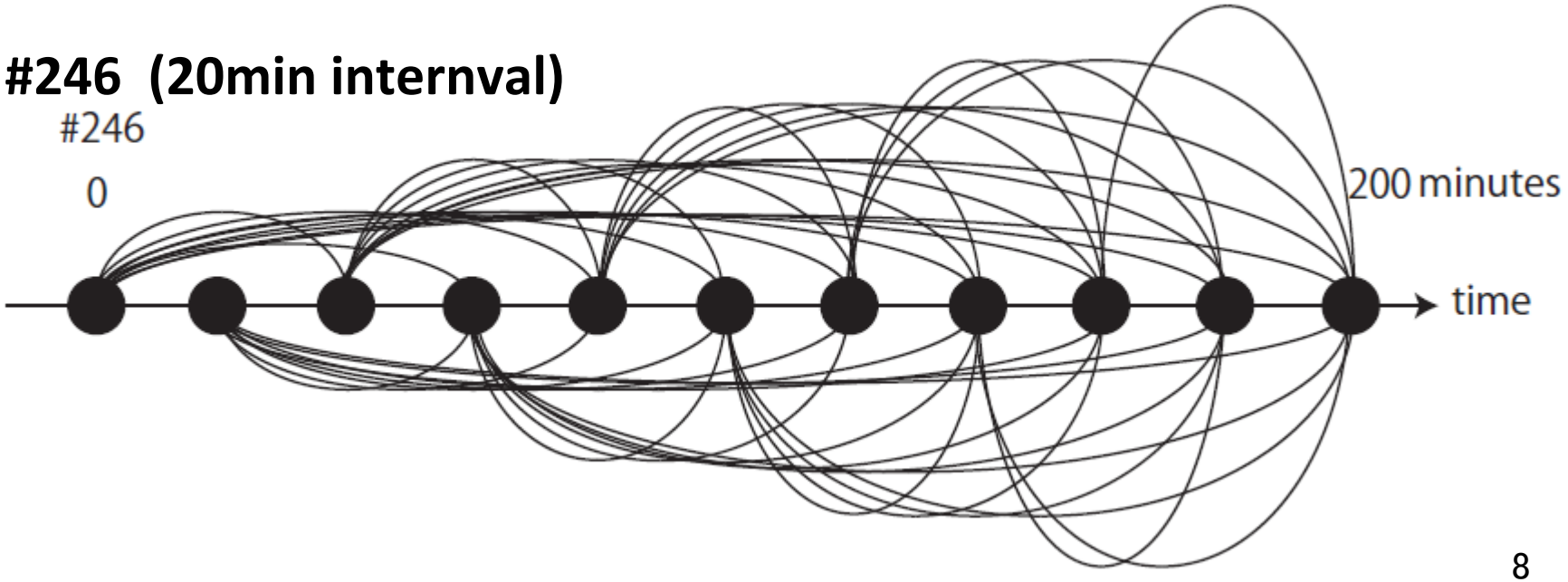

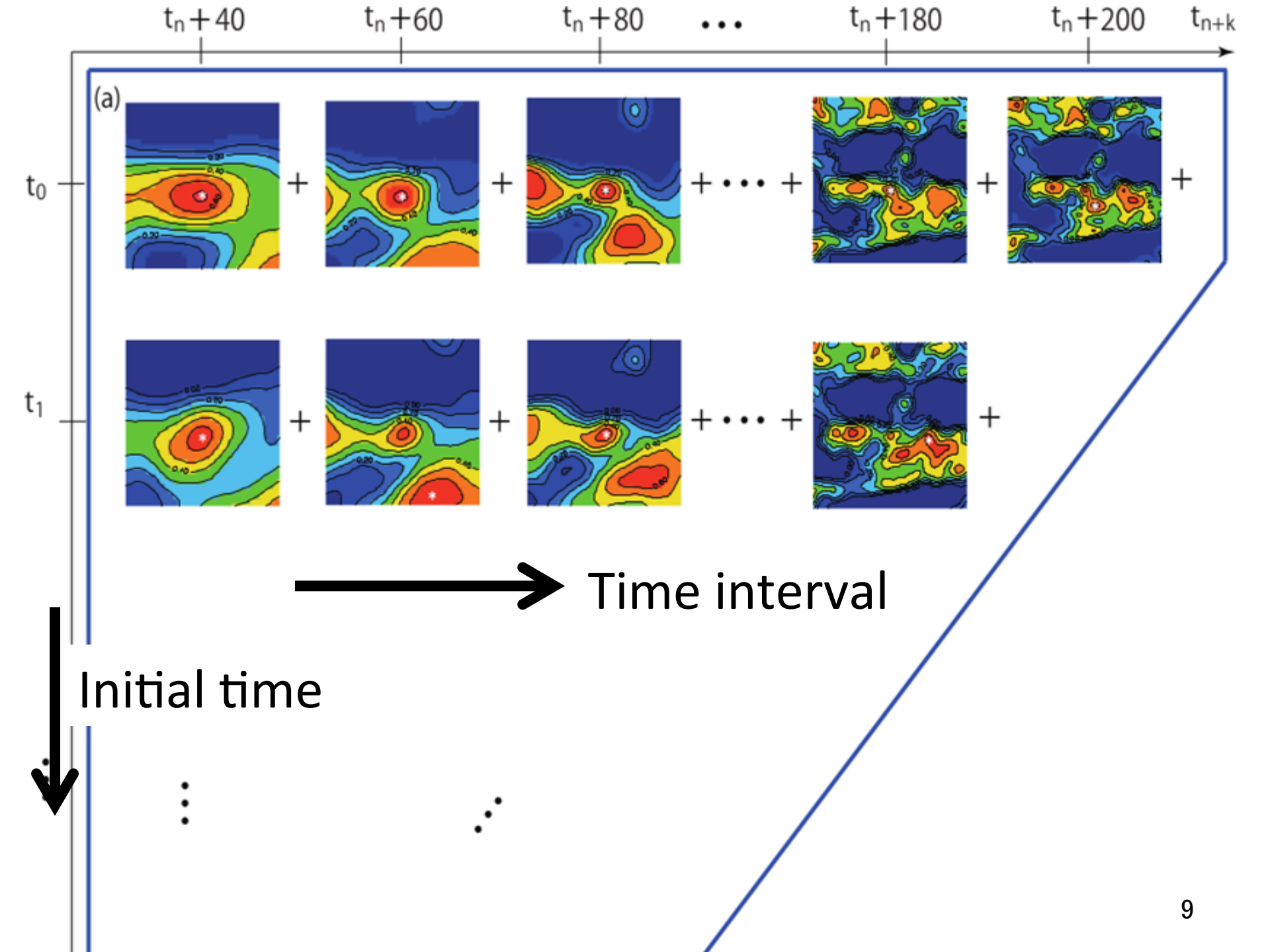
t_n+40
t_n+60
t_n+80
t_n+180
t_n+200
t_{n+k}
(a)
t_0
t_1
Time interval
Initial time

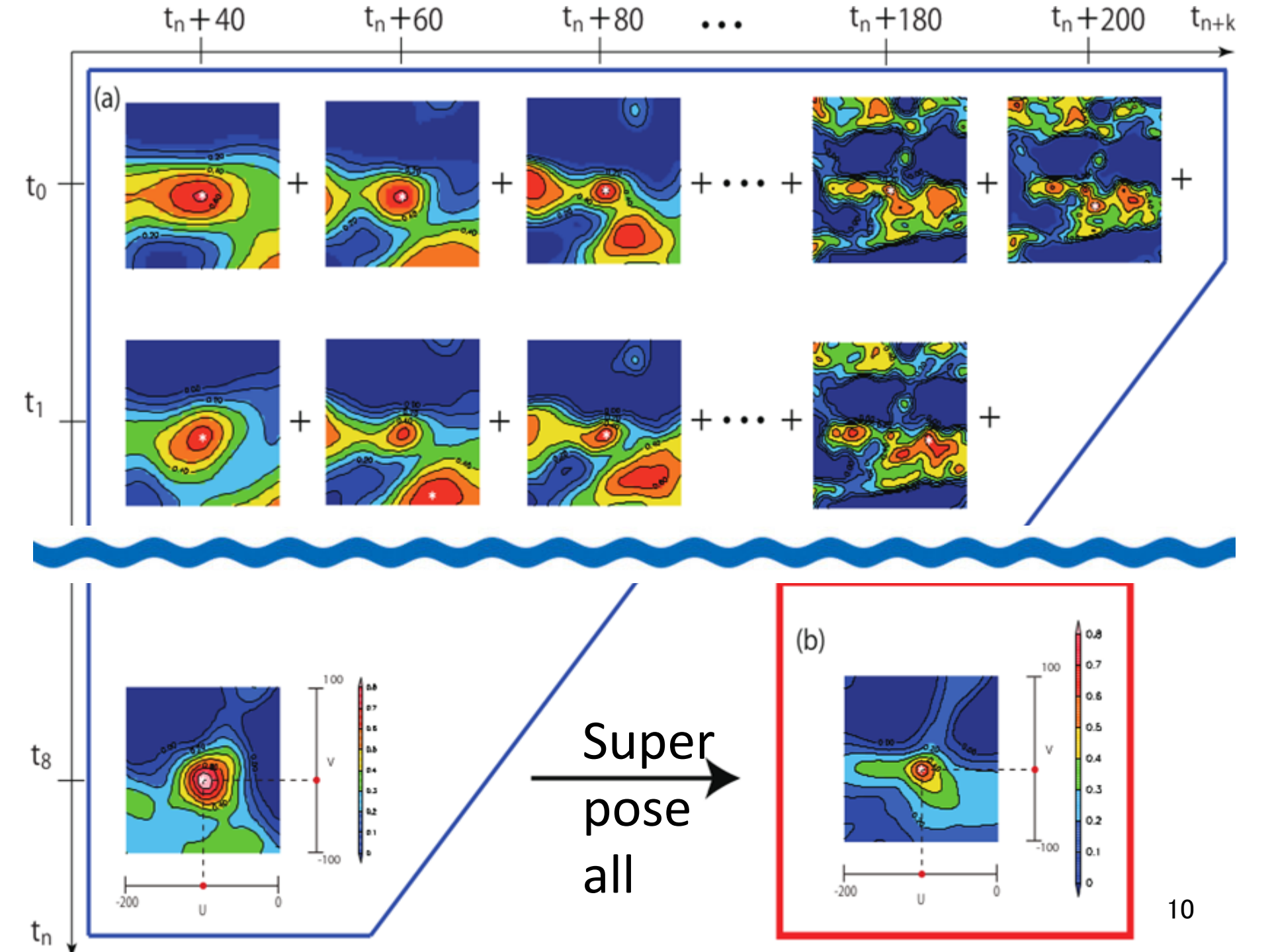
t_n+40
t_n+60
t_n+80
...
t_n+180
t_n+200
t_{n+k}
(a)
t_0
t_1
t_8
t_n
100
V
-100
-200
U
0
Super
pose
all
(b)
0.8
0.7
0.6
0.5
0.4
0.3
0.2
0.1
0

Δ*t* greater ⇒ Search region wider

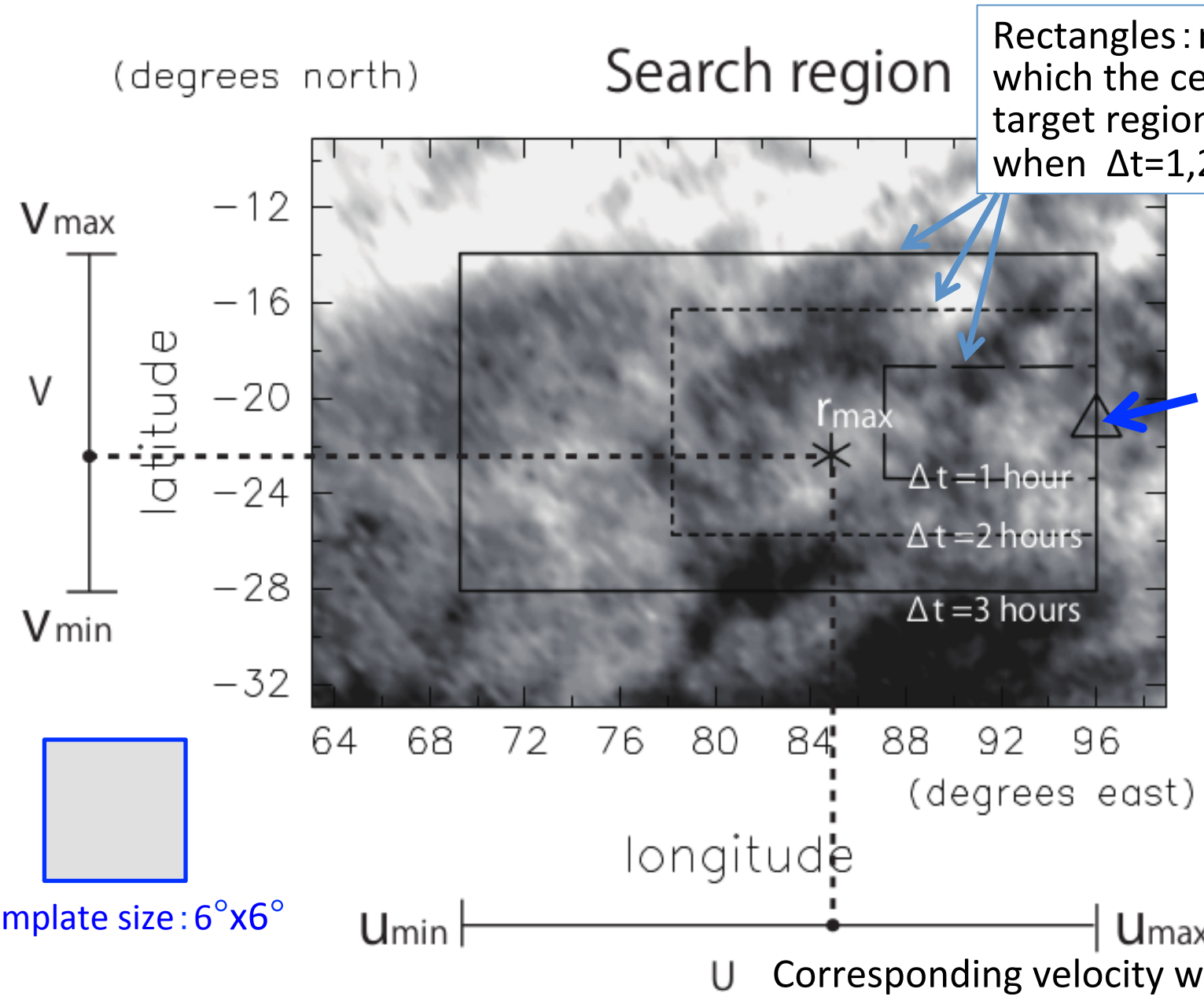

Essence of the CC superposition

$$r(x,y,t)=1/P\sum(t\downarrow 1,t\downarrow 2)\uparrow\blacksquare\langle f\uparrow' (x+u\,t\downarrow 1, y+v\,t\downarrow 1, t+t\downarrow 1) f'(x+u\,t\downarrow 2, y+v\,t\downarrow 2, t+t\downarrow 2)\rangle$$

- $\langle\ \rangle$: average over small *x*&*y* ranges (6°x 6° in IH15)
- P : the number of the $(t\downarrow 1, t\downarrow 2)$ combinations
- $f\uparrow'$: normalized brightness deviation
- u and v : the velocity to be derived.

(Traditional one-pair method: $P=1$ & $t\downarrow 1=0$, $t\downarrow 2=\Delta t$)

Why does the superposition enhance (reduce) the correct (wrong) peak(s)?

- For match with actual similar features
  - Suppose cloud features A around (x,y) and B around $(x+c,y+d)$ that are similar at $t=t↓0$, and they are advected by (u,v) (assume a common velocity, since they are nearby)
  - Correlation between A at $t↓0$ and B at $t↓0+\Delta t$ → peaks at velocity = $(u+c/\Delta t, v+d/\Delta t)$
    - Varies by Δt unless $c=d=0$ → peak reduced ($c=d=0$ means correct match)
    - Point: to have various Δt values
- Match by noise or error
  - is also reduced by superposition, if noise/error is independent among images (regardless Δt values)

Why does the superposition increase the accuracy too?

- Because it reduces the random peak shift by noise and pixel discretization

The $1/\sqrt{N}$ effect

Spatial superposition (~running mean) of CC surfaces (additional; STS in IH15)

- Adequate when the desired spatial resolution is coarser than the template size.
- Overlay the 5 CC surfaces (after the superposition in time domain) before deriving velocity
  - Trade off between spatial resolution and accuracy
  - **The default** procedure in IH15 (used in what follows)

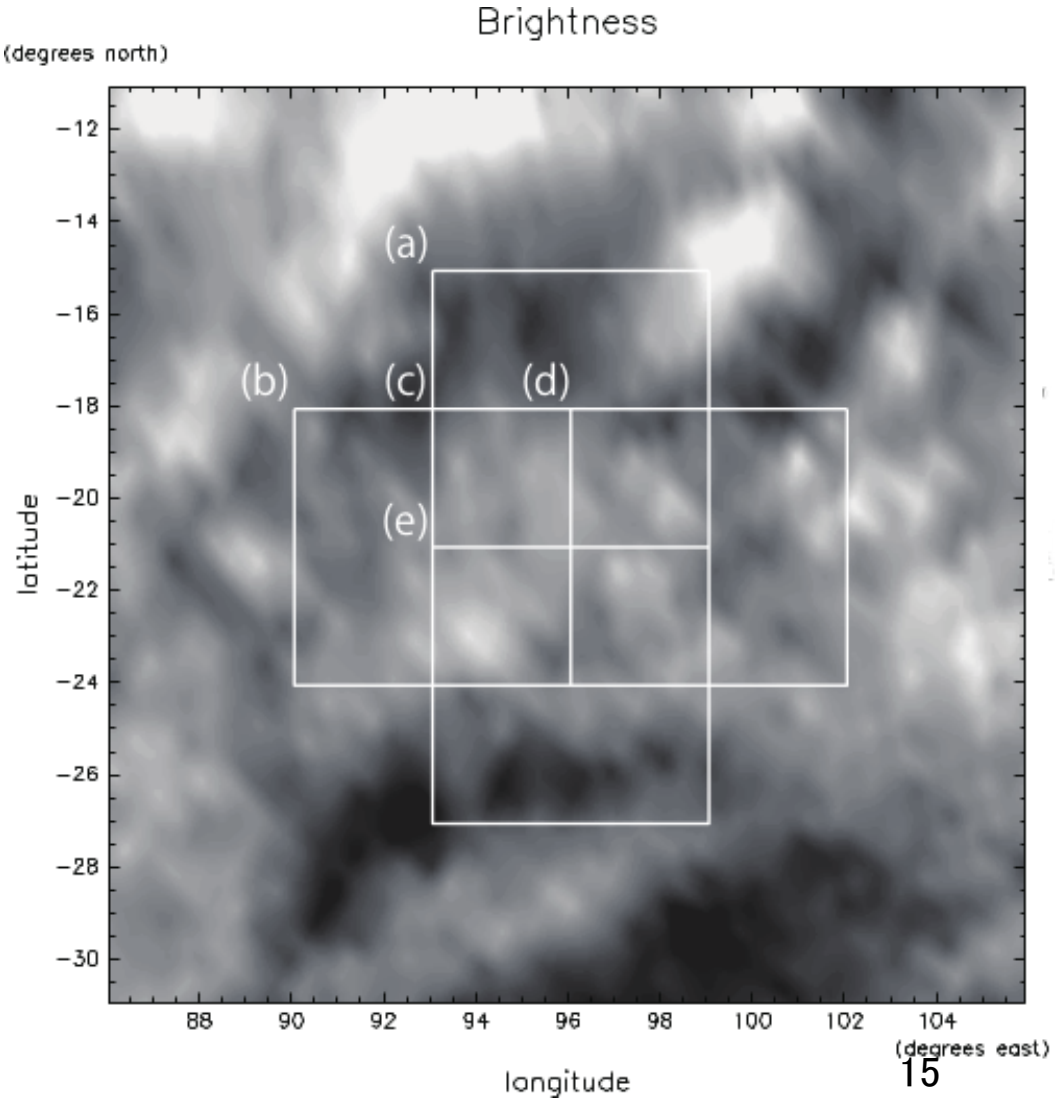

Error estimation: Necessity

- **Crucial!** Needed to judge what we can do (to what extent) with the data!
- Let's consider physical properties of horizontal winds and Venusian cloud morphology.
  - Horizontal wind spectra are expected to be red → error level sets the effective resolution.
  - Clouds are some times featureless: accuracy varies significantly, so the "representative" error is helpful only for statistics.
- In previous studies: use σ (std.dev.; e.g. against zonal mean). Since $\langle \sigma^2 \rangle = \langle \sigma_{\mathrm{natural}}^2 \rangle + \langle \sigma_{\mathrm{err}}^2 \rangle$, it's safe to use σ, but it is useless as a measure of error if $\langle \sigma_{\mathrm{err}}^2 \rangle \ll \langle \sigma_{\mathrm{natural}}^2 \rangle$, although to achieve it is what we need to study atmospheric disturbances.

Error evaluation 1 (precision)

- Utilize the lower confidence bound (idea from Murachi, M-thesis, but significantly improved)
- In IH15
  - Use the effective (not nominal) degree of freedom formulated for the superposed CC.
  - Covers streaky clouds（CC surfaces get also streaky）
    - Remark: precision is anisotropic (high in perpendicular directions). One can derive only 1D motion from a pure streak.
  - Applicable to one-pair estimates
  - Cannot tell anything about peak selection (drawback)

CC surface above the lower confidence bound (90%) is fit by

1. Elliptic paraboloid (for slantwise streaks)
2. Parabolas along cross sections at peak along u and v axes

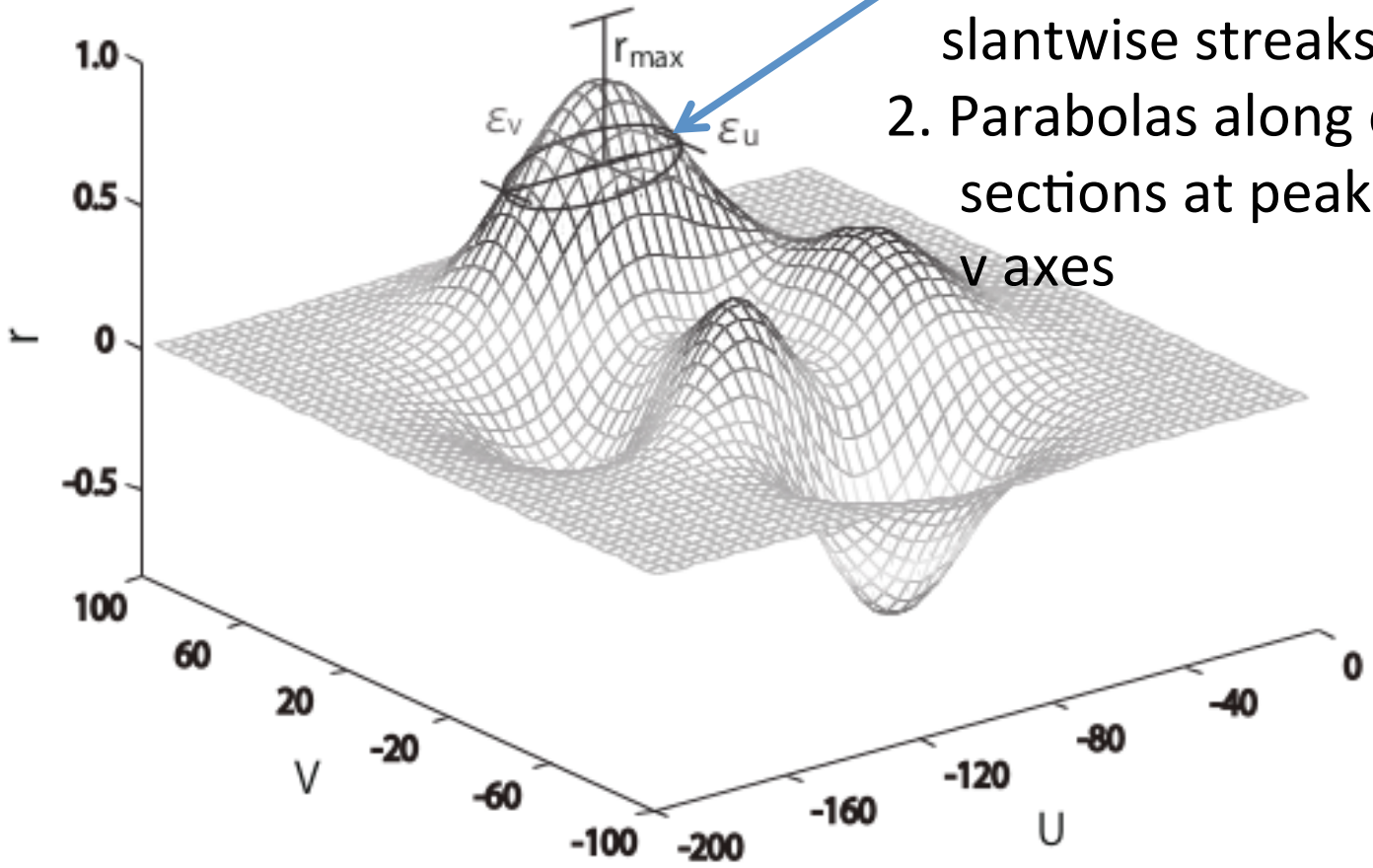

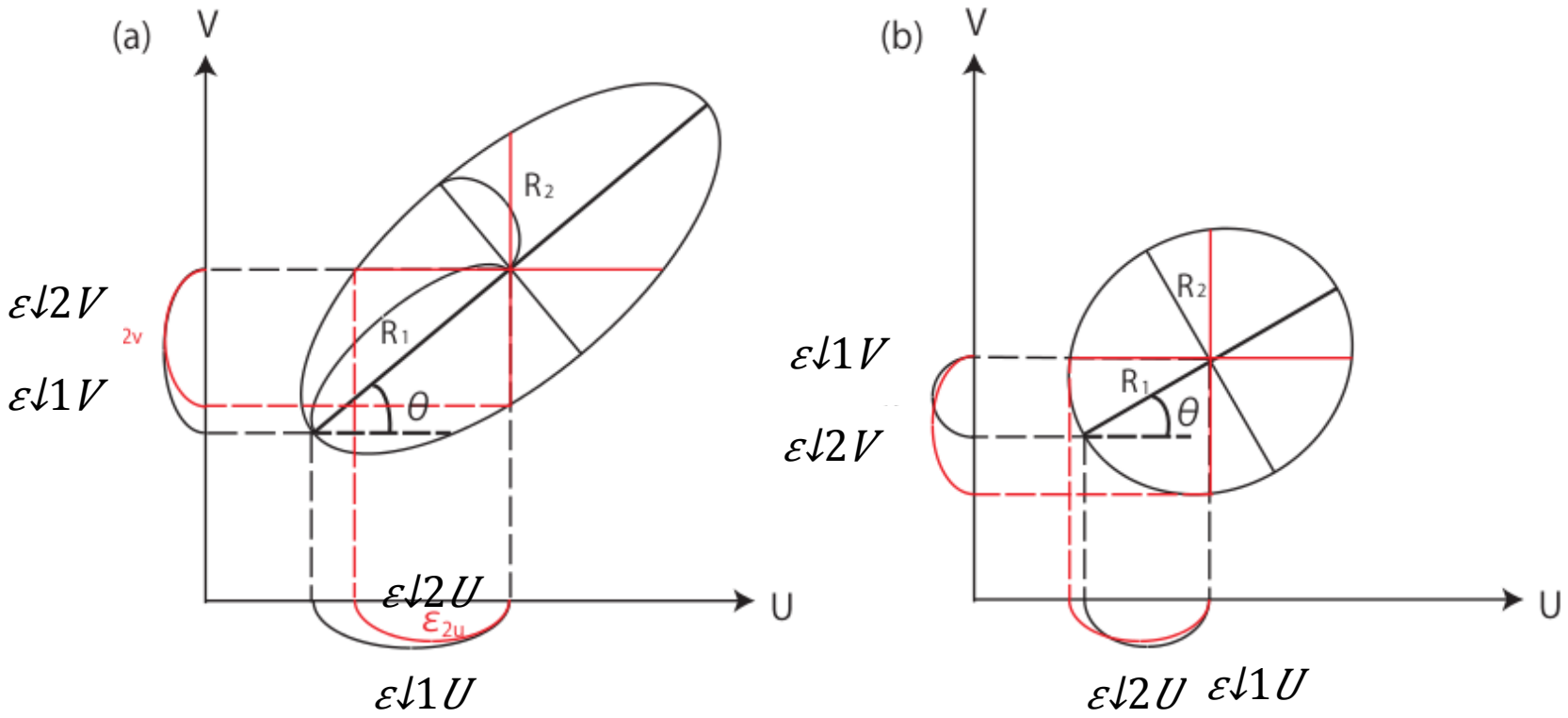

$\varepsilon = \max(\varepsilon\downarrow 1U, \varepsilon\downarrow 1V, \varepsilon\downarrow 2U, \varepsilon\downarrow 2U)$: the worst of the four params.

Caveat: confidence percentage (90%, here) is only applicable to CC.
Cannot be converted to the confidence level of (*u,v*).
But ε may be used as a relative measure of the precision of (*u,v*).

Error evaluation 2

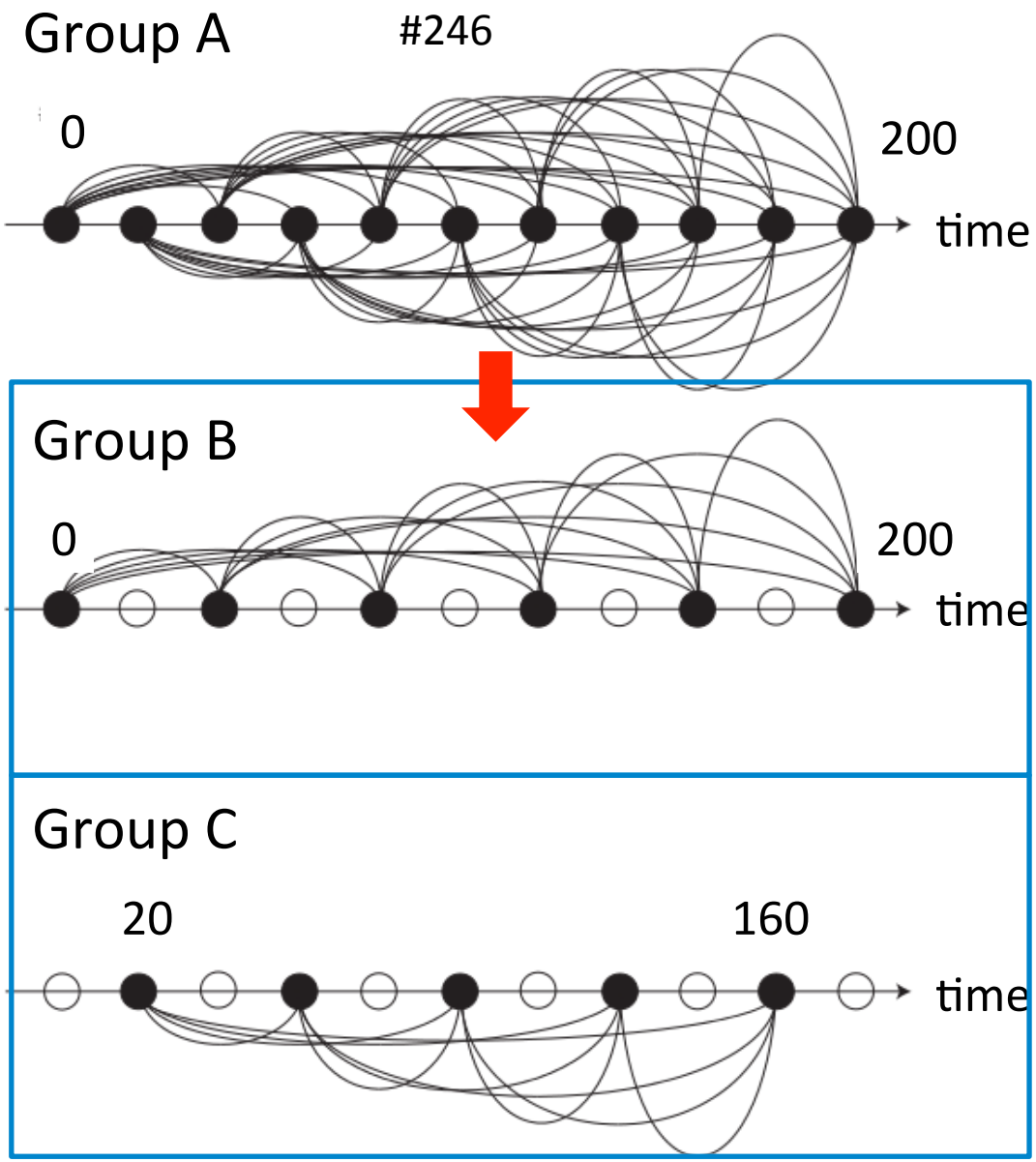

- Entire images (A) are divided into 2 groups (B,C) and winds are estimated from each
  - Use the rms between the two.
  - Note: B & C are expected to have greater error than A, since the number of pairs are smaller

absolute values of vector differences as

From IH15

$$\sigma_X(\lambda_a,\phi_b) \equiv \sqrt{\{u_t(\lambda_a,\phi_b)-u_X(\lambda_a,\phi_b)\}^2+\{v_t(\lambda_a,\phi_b)-v_X(\lambda_a,\phi_b)\}^2} \quad \text{for } X=\mathrm{A},\mathrm{B},\mathrm{C}, \tag{22}$$

and

$$\sigma_{\mathrm{BC}}(\lambda_a,\phi_b) \equiv \sqrt{\{u_{\mathrm{B}}(\lambda_a,\phi_b)-u_{\mathrm{C}}(\lambda_a,\phi_b)\}^2+\{v_{\mathrm{B}}(\lambda_a,\phi_b)-v_{\mathrm{C}}(\lambda_a,\phi_b)\}^2}. \tag{23}$$

If we assume that CMVs derived from a single pair has error with a normal distribution and the error is independent among pairs, we can expect the following relations:

$$\langle\sigma_{\mathrm{B}}^2\rangle = \frac{P}{P_{\mathrm{B}}}\langle\sigma_{\mathrm{A}}^2\rangle, \tag{24}$$

$$\langle\sigma_{\mathrm{C}}^2\rangle = \frac{P}{P_{\mathrm{C}}}\langle\sigma_{\mathrm{A}}^2\rangle, \tag{25}$$

$$\langle\sigma_{\mathrm{BC}}^2\rangle = \langle\sigma_{\mathrm{B}}^2\rangle+\langle\sigma_{\mathrm{C}}^2\rangle, \tag{26}$$

(P, P_{A}, P_{B} : the number of pairs in the groups A,B,C)

⇒ Expected error (here, the factor of 1.96 is for the 95% confidence level)

$$\chi(\lambda_a,\phi_b) \equiv 1.96\left(\frac{P}{P_{\mathrm{B}}}+\frac{P}{P_{\mathrm{C}}}\right)^{-\frac{1}{2}}\sigma_{\mathrm{BC}}(\lambda_a,\phi_b)$$

Characteristics of χ

- Direct (not indirect) measure of errors in (*u*, *v*)
- Deals with peak selection, but only partially
  (peaks in B and C may differ, though agreement does not guarantee correctness).

Screening

- Made by
  1. Peak CC value: $r_{max} \geq 0.6$
  2. Mapped CC lower bound: $\varepsilon \leq 20$ m/s
  3. Error form 2-group comparison: $\chi \leq 10$ m/s
- No correction of erroneous vectors (can be introduced, but simply not have been tried)

Result example (Orbit 246)

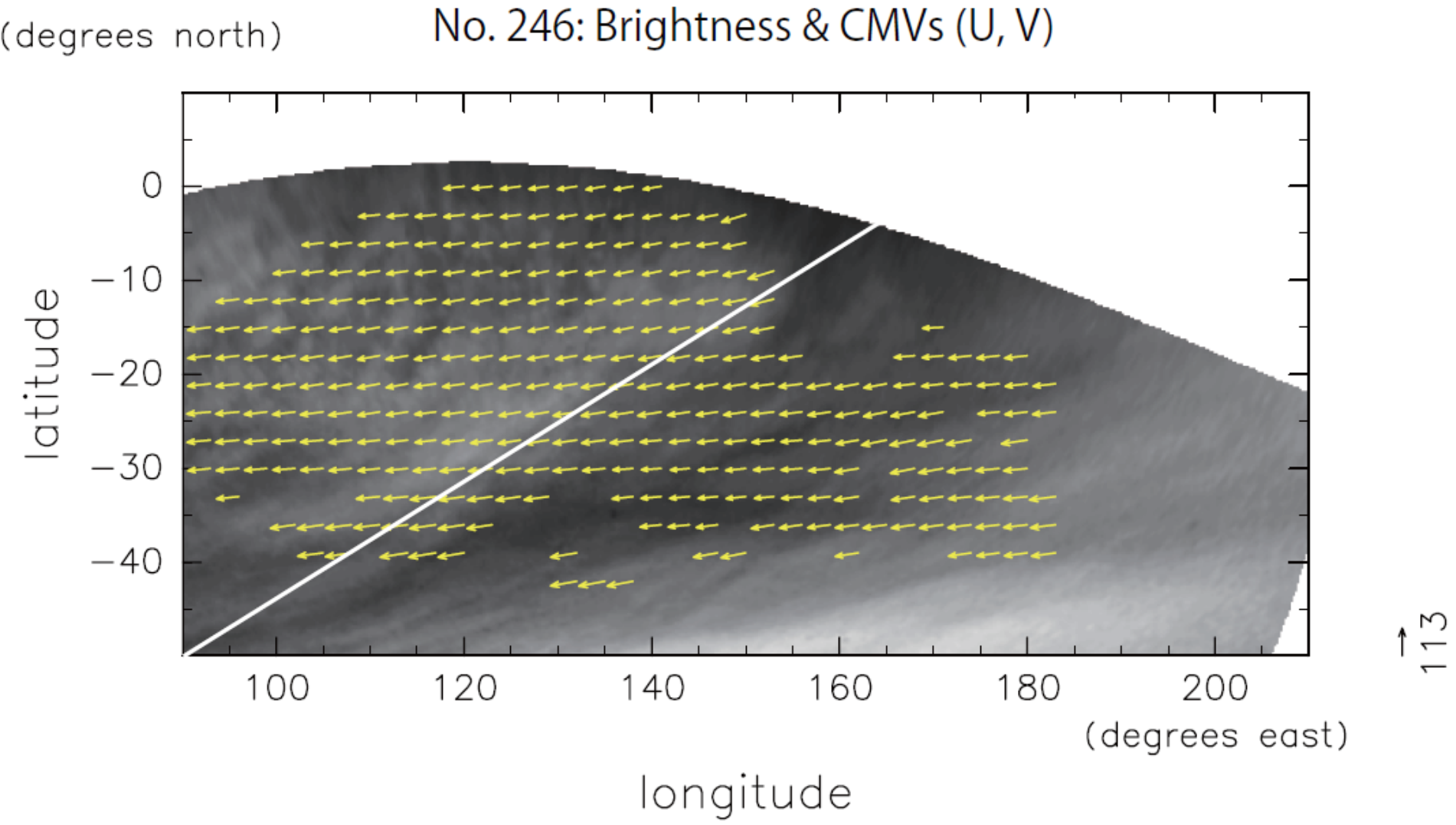

Our estimation is limited down to 45°S

Added a uniform zonal flow: (90,0) m/s

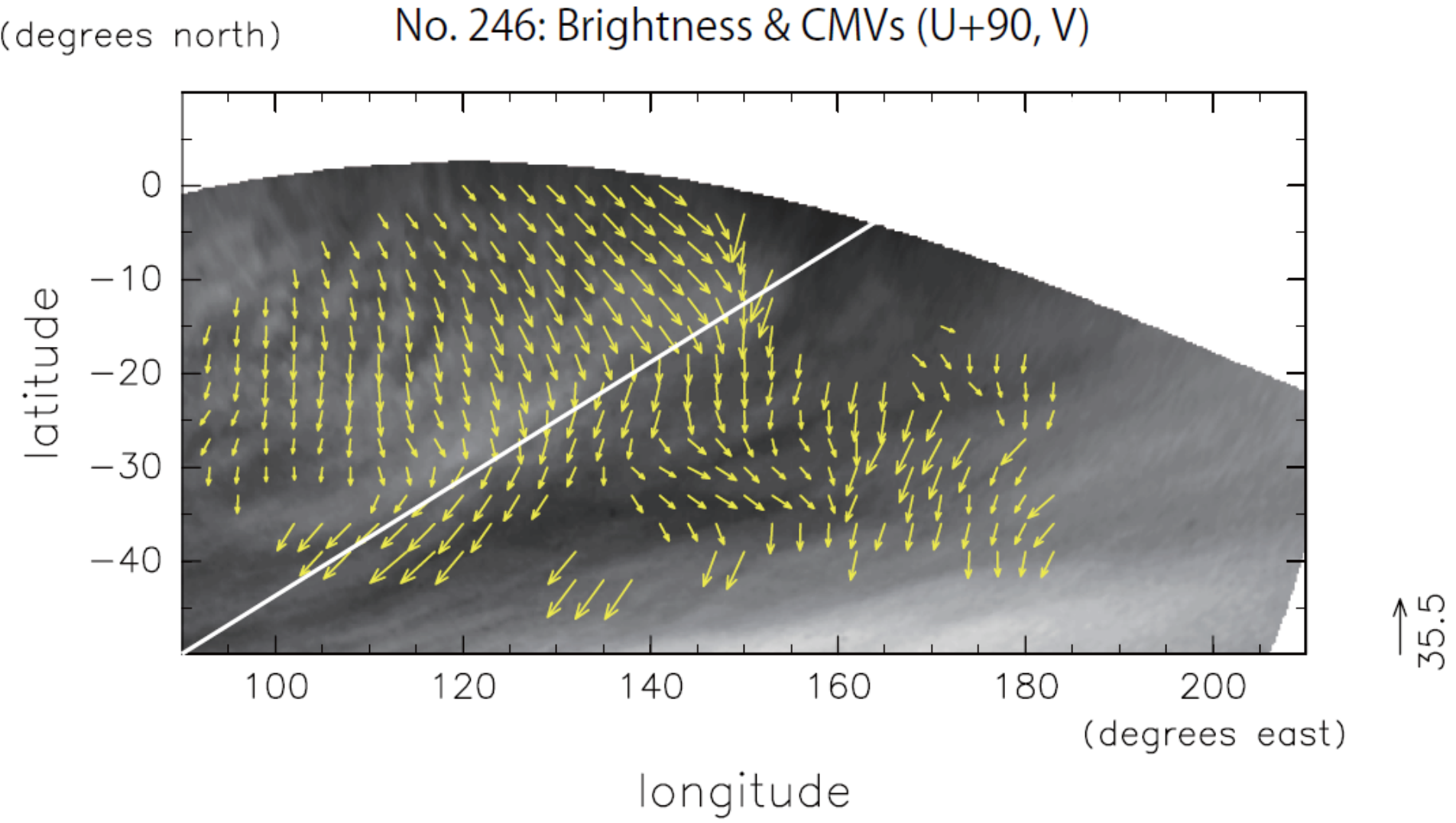

Ref : Kouyama et al (2012) Example of wind from Galileo images (violet)

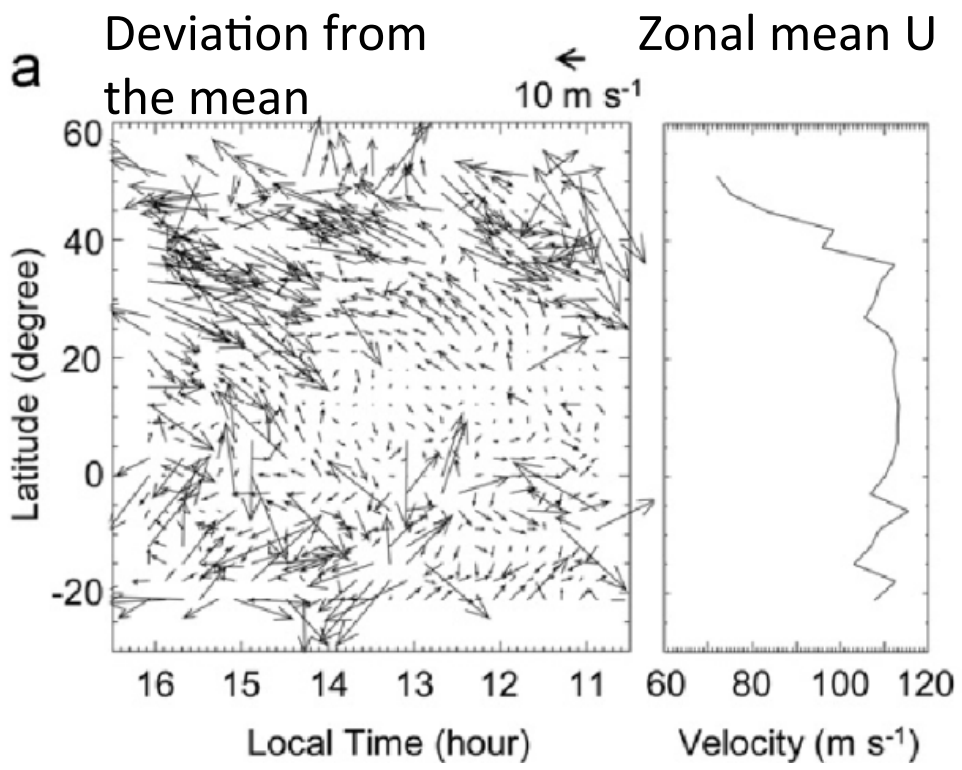

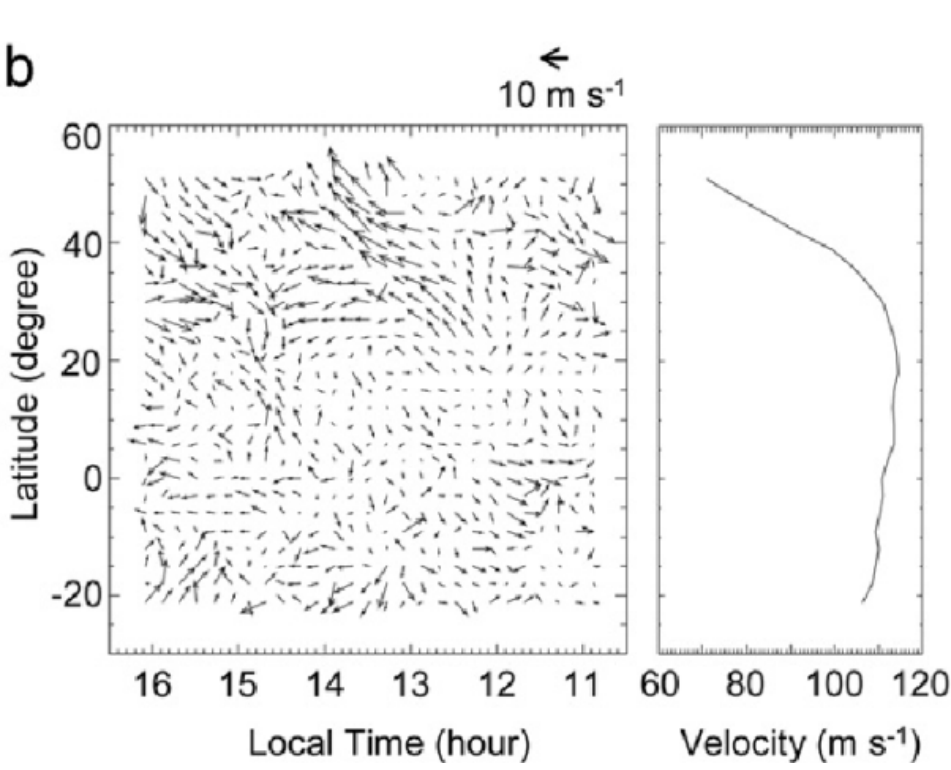

Simple CC

Corrected by selecting peaks

Error evaluation

(#246)

Max CC r_{max}

Mapped CC lower bound ε

Error from 2-group comparison χ

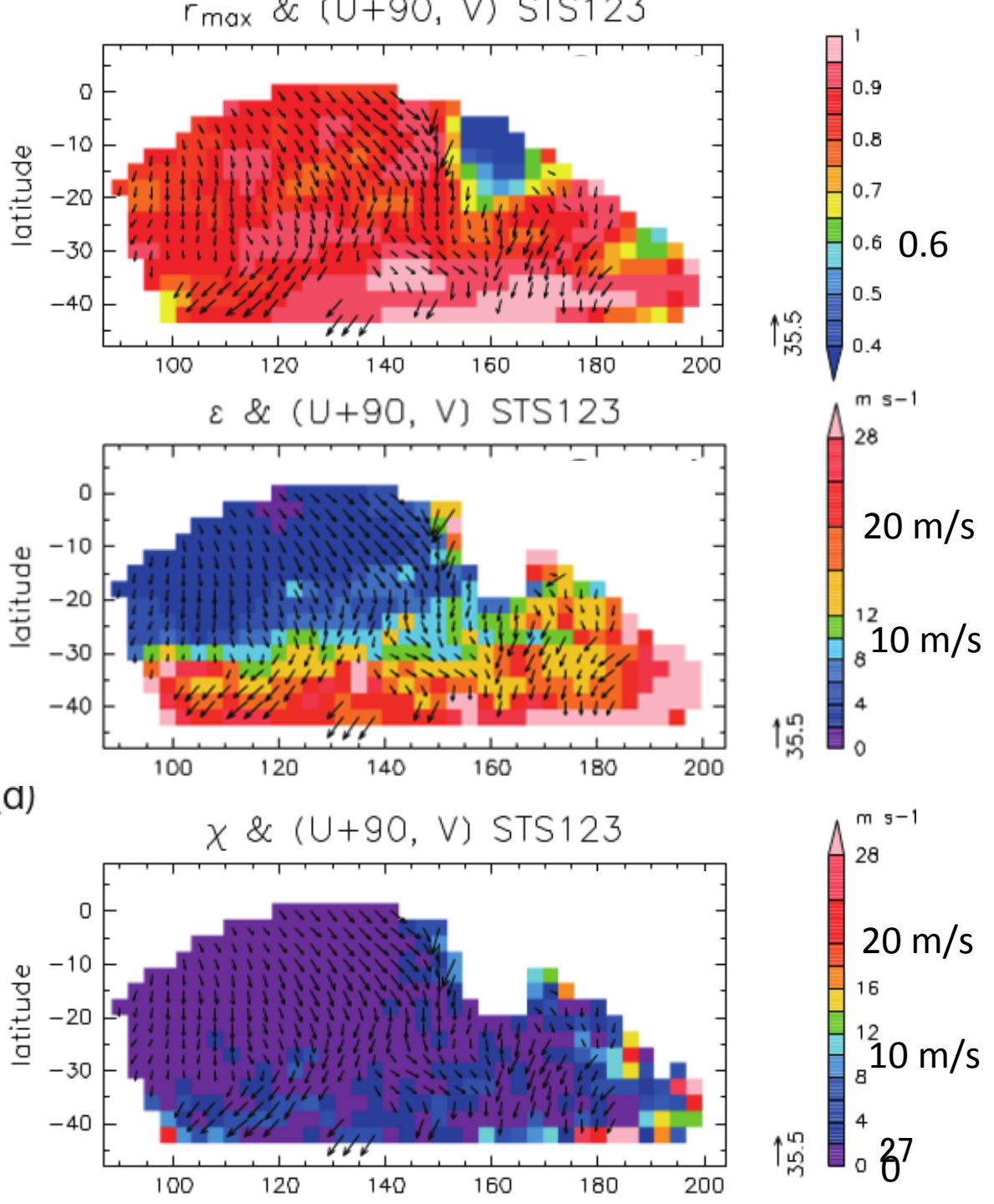

(a)

Screened on by r_{max}

div & rot

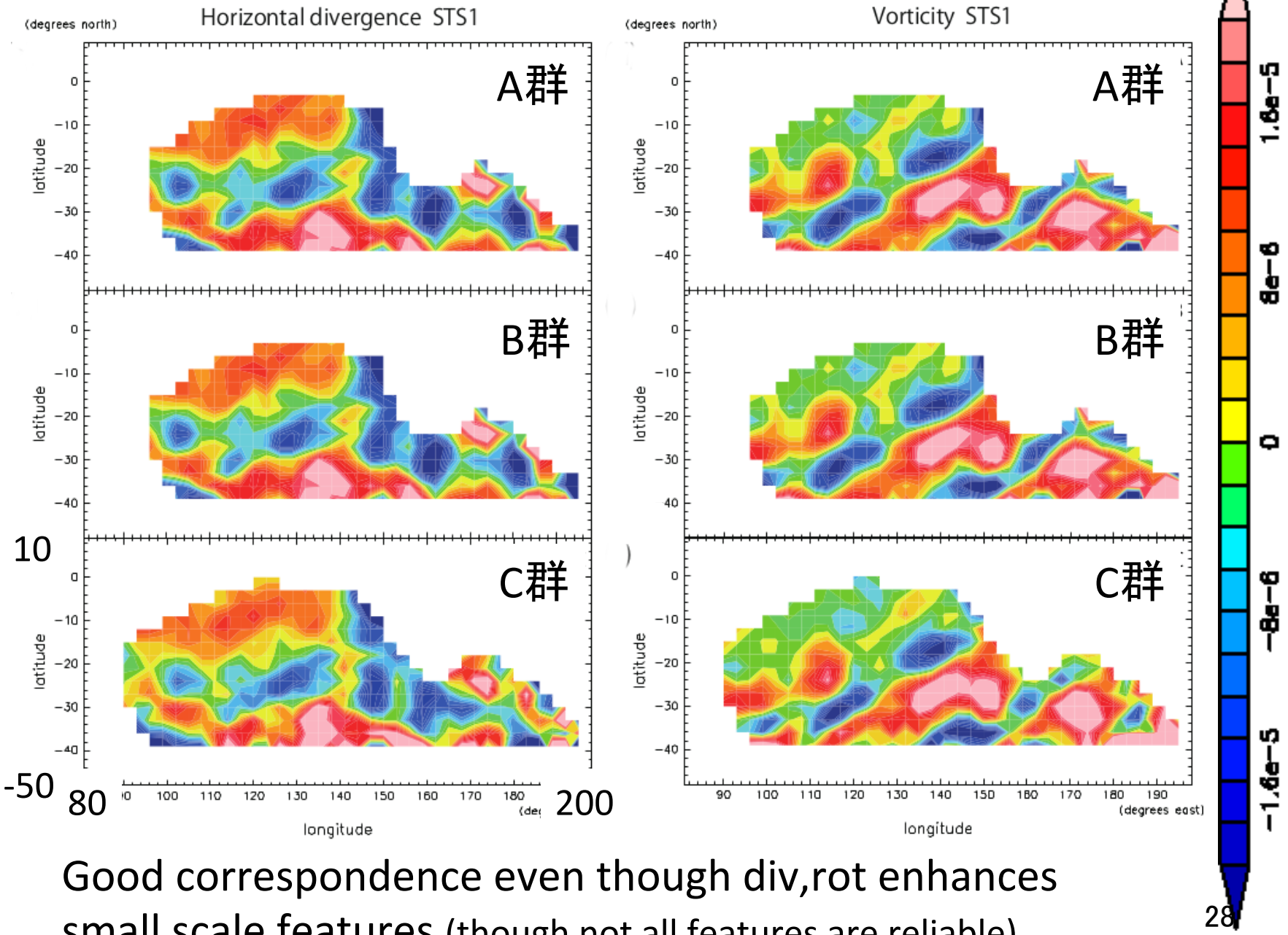

Good correspondence even though div,rot enhances small scale features (though not all features are reliable)

Summary of the error estimates（After the screening. Orbits 243-267）

χ (from 2-group diff.)

	low latitude		mid latitude	
	rms value	median value	rms value	median value
wind velocity (χ)	2.4 m s^{-1}	1.5 m s^{-1}	3.0 m s^{-1}	2.0 m s^{-1}
horizontal divergence (χ_δ)	7.7×10^{-6} s^{-1}	2.9×10^{-6} s^{-1}	1.8×10^{-5} s^{-1}	6.4×10^{-6} s^{-1}
vorticity (χ_ζ)	7.8×10^{-6} s^{-1}	3.0×10^{-6} s^{-1}	1.6×10^{-5} s^{-1}	5.3×10^{-6} s^{-1}

ε (from CC confidence)

accuracy evaluation	low latitude		mid latitude	
	rms value	median value	rms value	median value
statistical accuracy	9.4 m s^{-1}	7.8 m s^{-1}	14.8 m s^{-1}	15.0 m s^{-1}

- In general, $\chi < \varepsilon$
- If measured by χ, typical error is 2 m/s. (Too good for manual (human-eye) verification. Q: actually good beyond the limit of manual tracking, or χ is too good?)
- Low lat (EQ-30S) better than mid lat (30S-45S)
- χ : median < rms（∵big values are outliers）

Results (#200s)

- 10 orbits from 243 to 267
  - Other orbits (in this period) are not available since the number of images ＜4
  - For each of the 10 orbits, 8-11 images are used.
  - Caveat (from subjective verification)：some results (vectors) are likely invalid beyond the χ value.

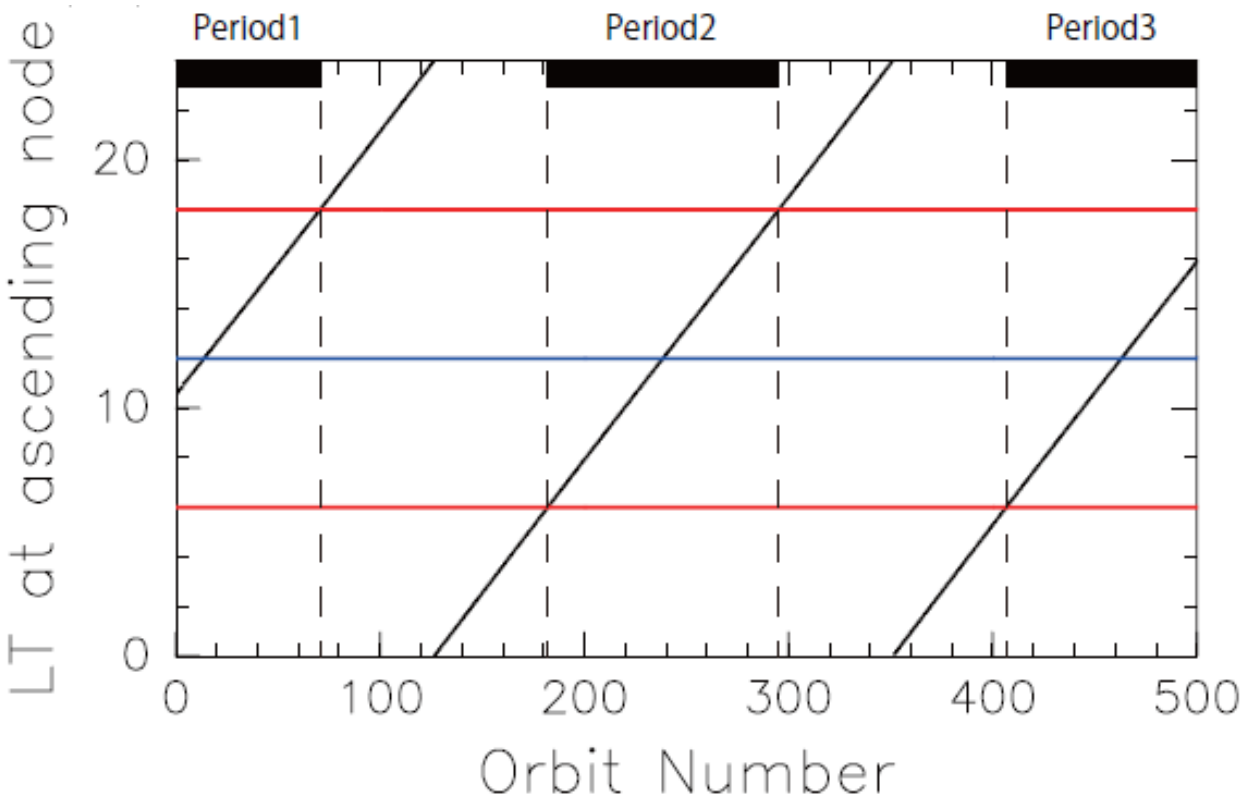

風速の水平分布（#243）

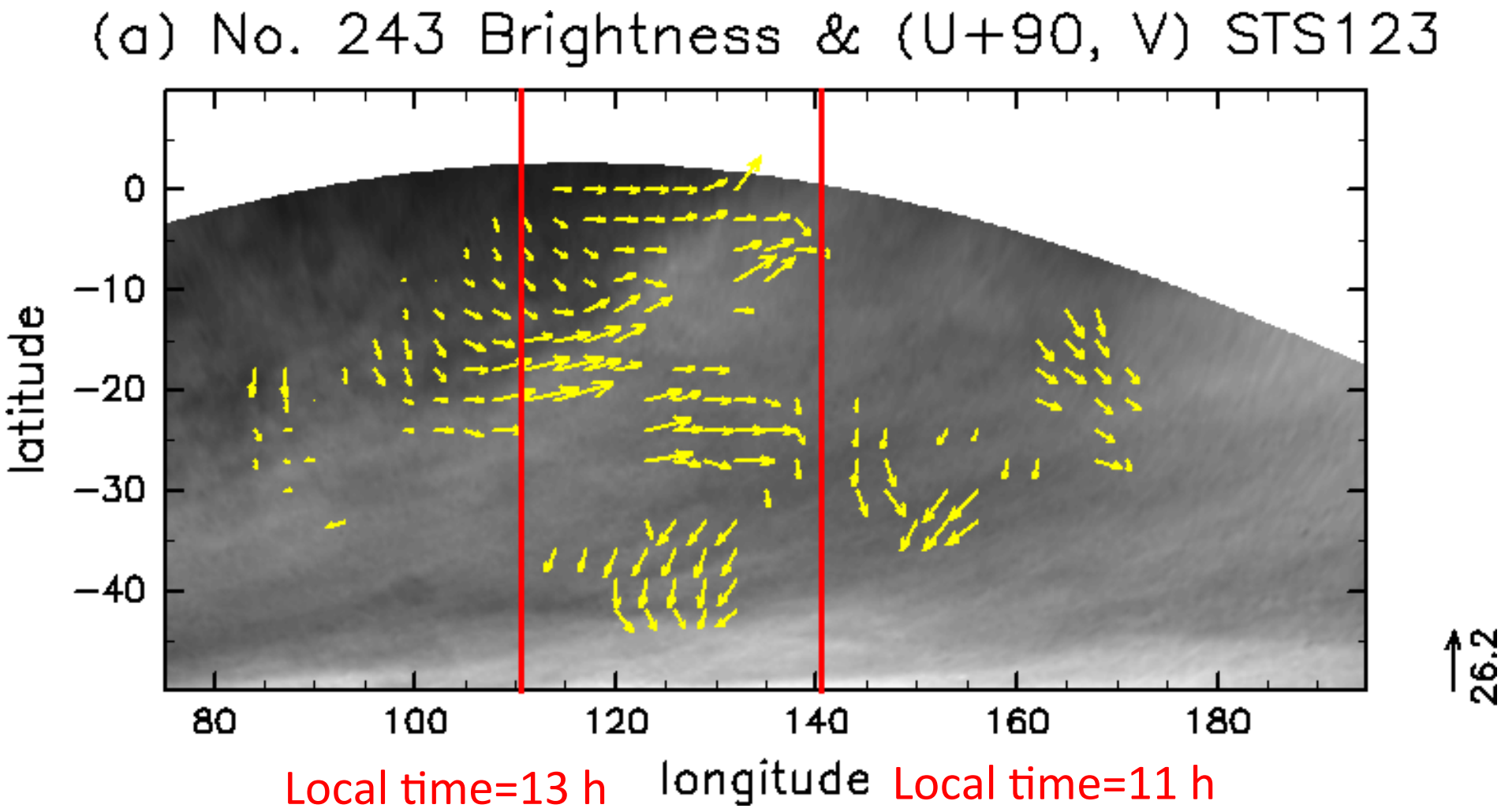
(a) No. 243 Brightness & (U+90, V) STS123
0
−10
−20
−30
−40
latitude
80
100
120
140
160
180
longitude
Local time=13 h
Local time=11 h
26.2

風速の水平分布（#246）

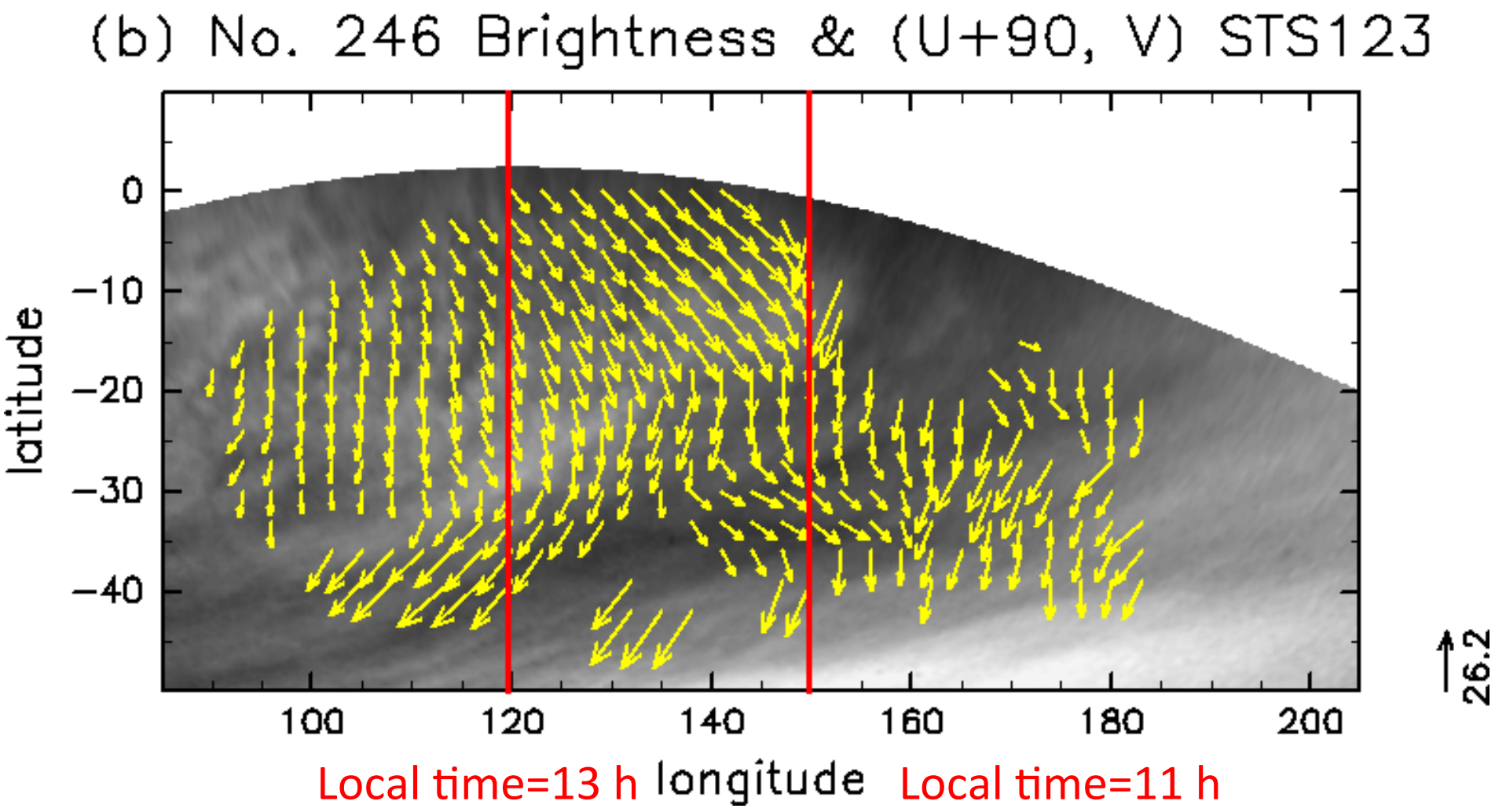
(b) No. 246 Brightness & (U+90, V) STS123
0
−10
−20
−30
−40
latitude
100
120
140
160
180
200
Local time=13 h
longitude
Local time=11 h
26.2

風速の水平分布（#250）

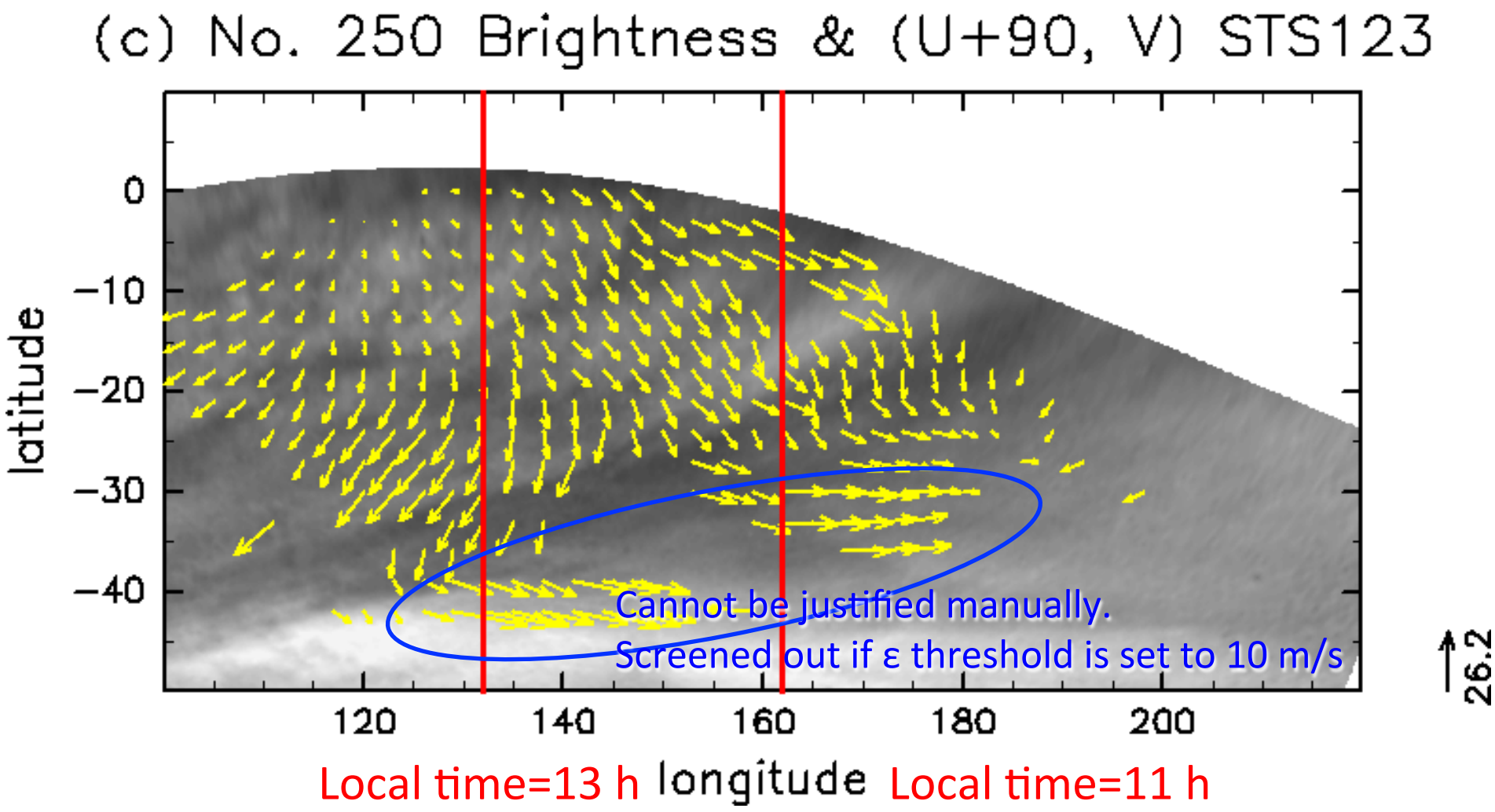
(c) No. 250 Brightness & (U+90, V) STS123
0
−10
−20
−30
−40
latitude
120
140
160
180
200
Local time=13 h
longitude
Local time=11 h
Cannot be justified manually.
Screened out if ε threshold is set to 10 m/s
26.2

風速の水平分布(#257)

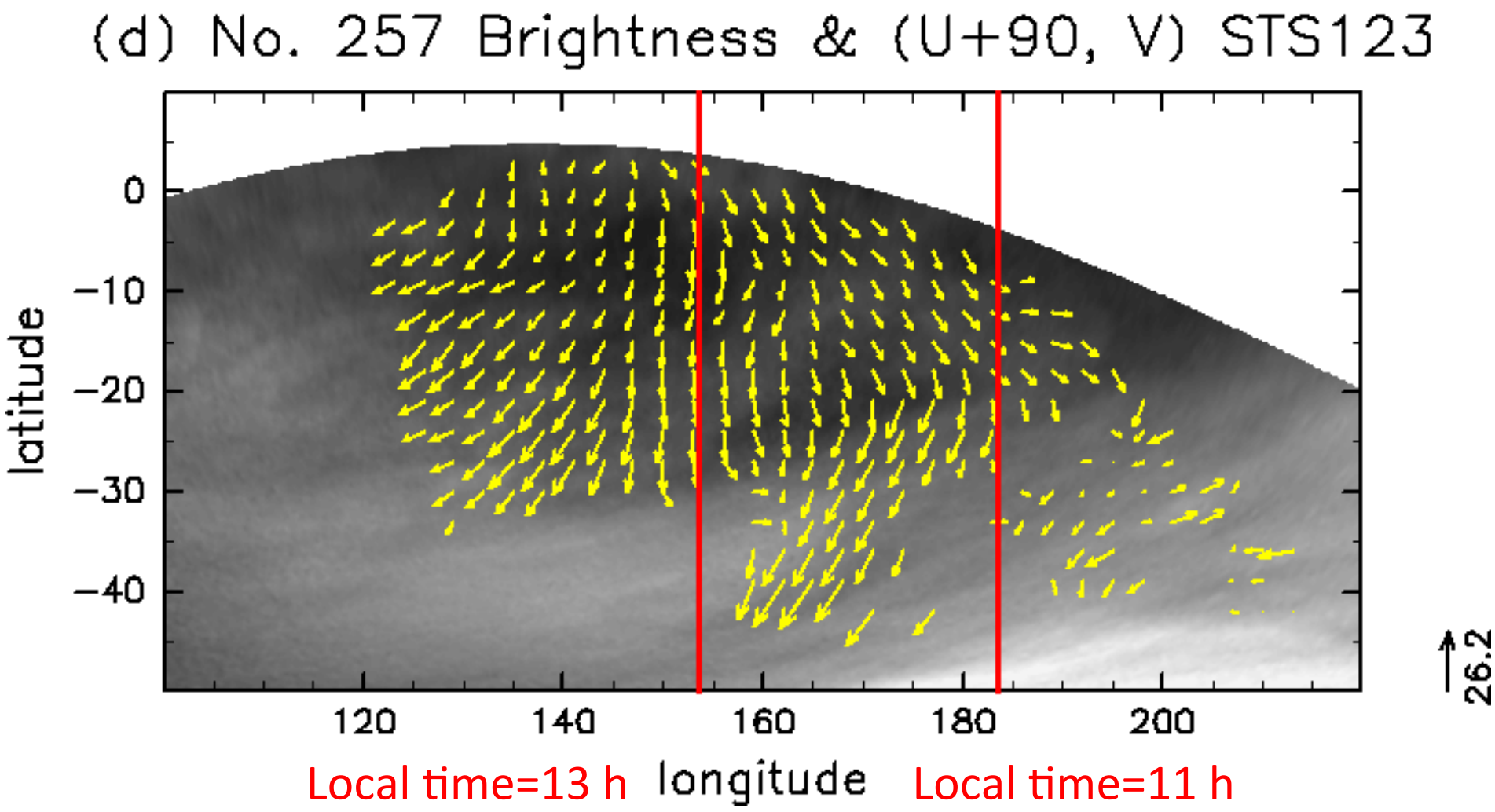
(d) No. 257 Brightness & (U+90, V) STS123
0
−10
−20
−30
−40
latitude
120
140
160
180
200
Local time=13 h
longitude
Local time=11 h
26.2

風速の水平分布(#258)

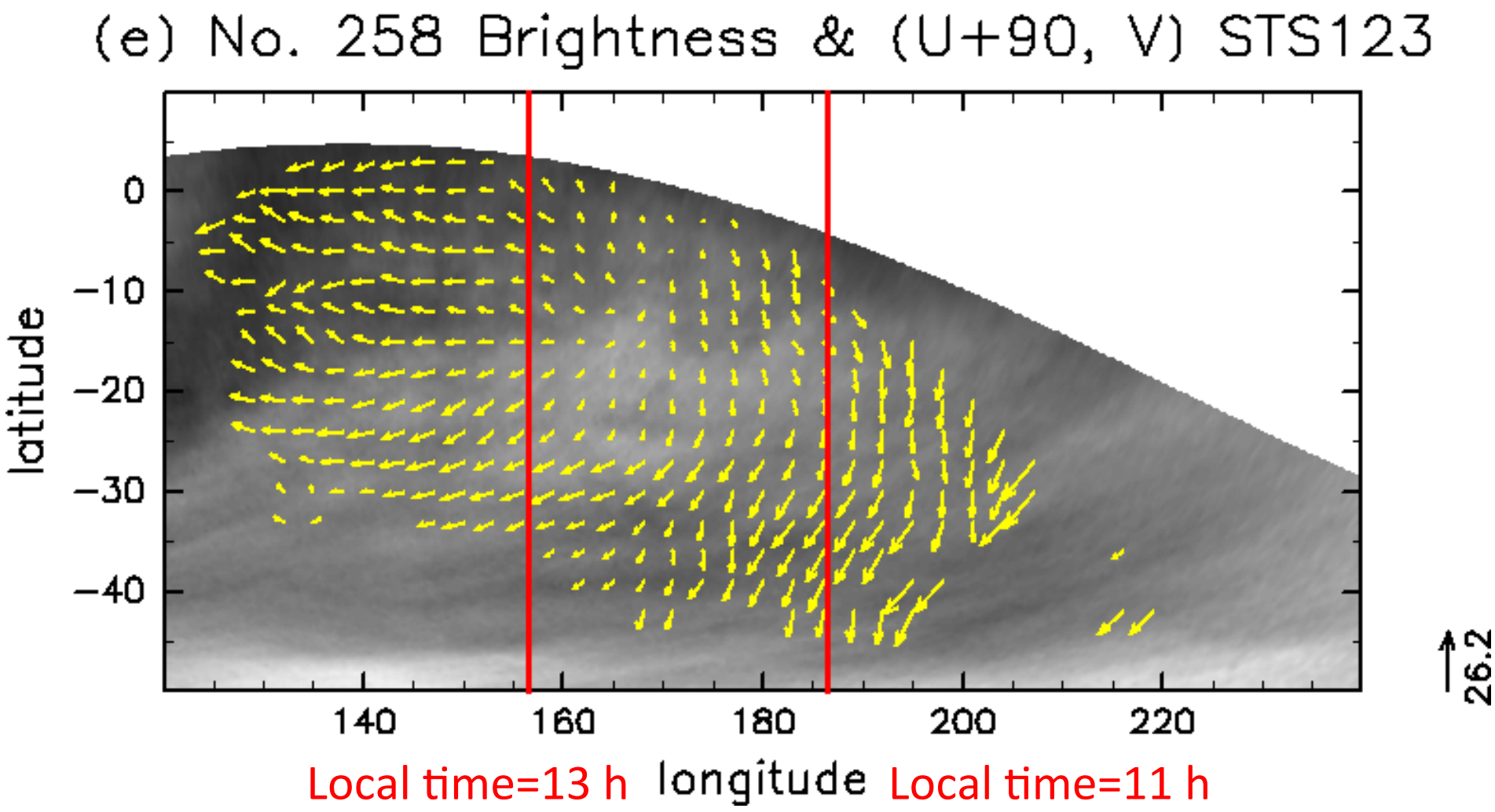
(e) No. 258 Brightness & (U+90, V) STS123
0
−10
−20
−30
−40
latitude
140
160
180
200
220
longitude
Local time=13 h
Local time=11 h
26.2

風速の水平分布（#260）

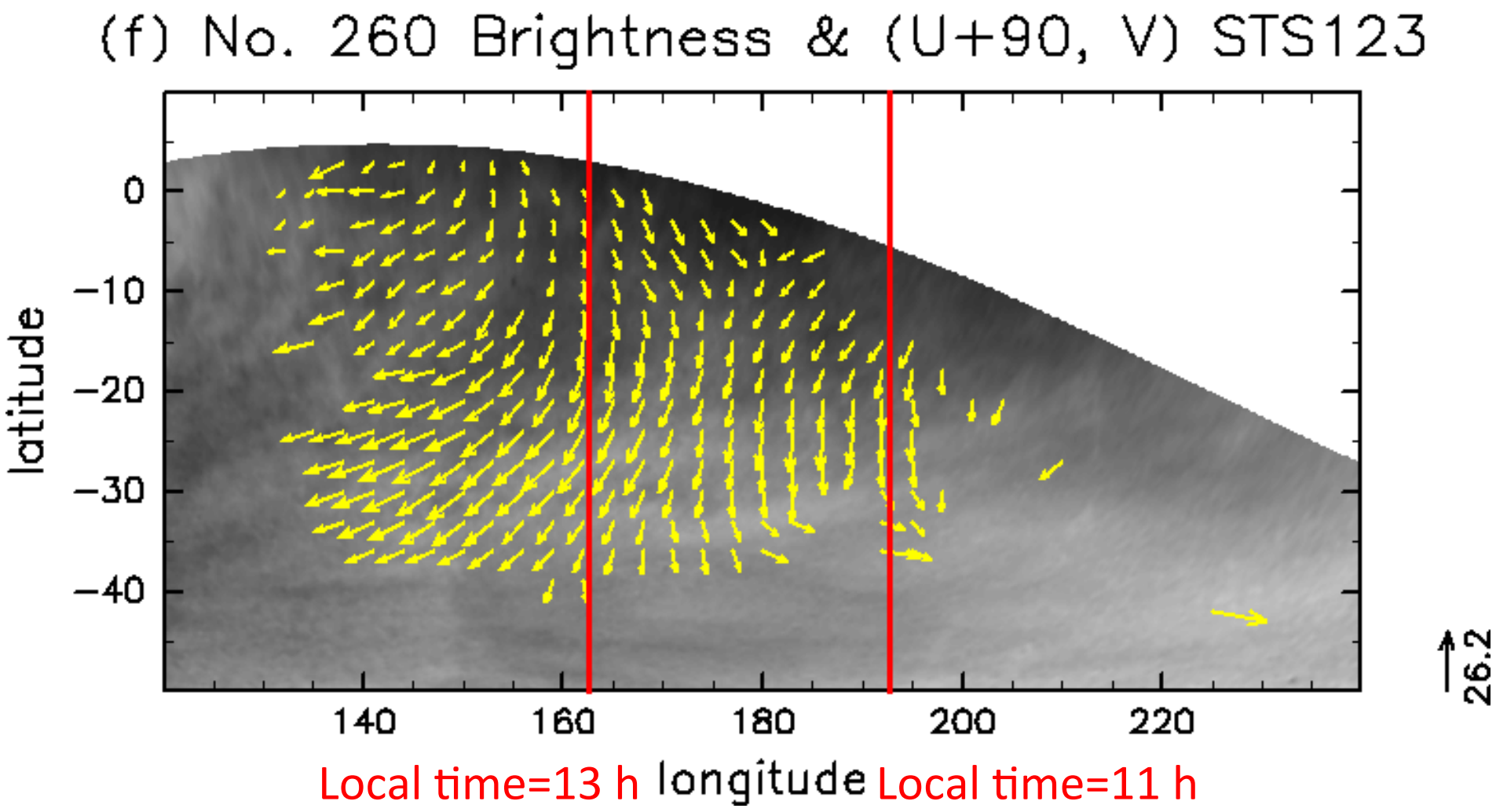
(f) No. 260 Brightness & (U+90, V) STS123
0
−10
−20
−30
−40
latitude
140
160
180
200
220
Local time=13 h
longitude
Local time=11 h
26.2

風速の水平分布（#263）

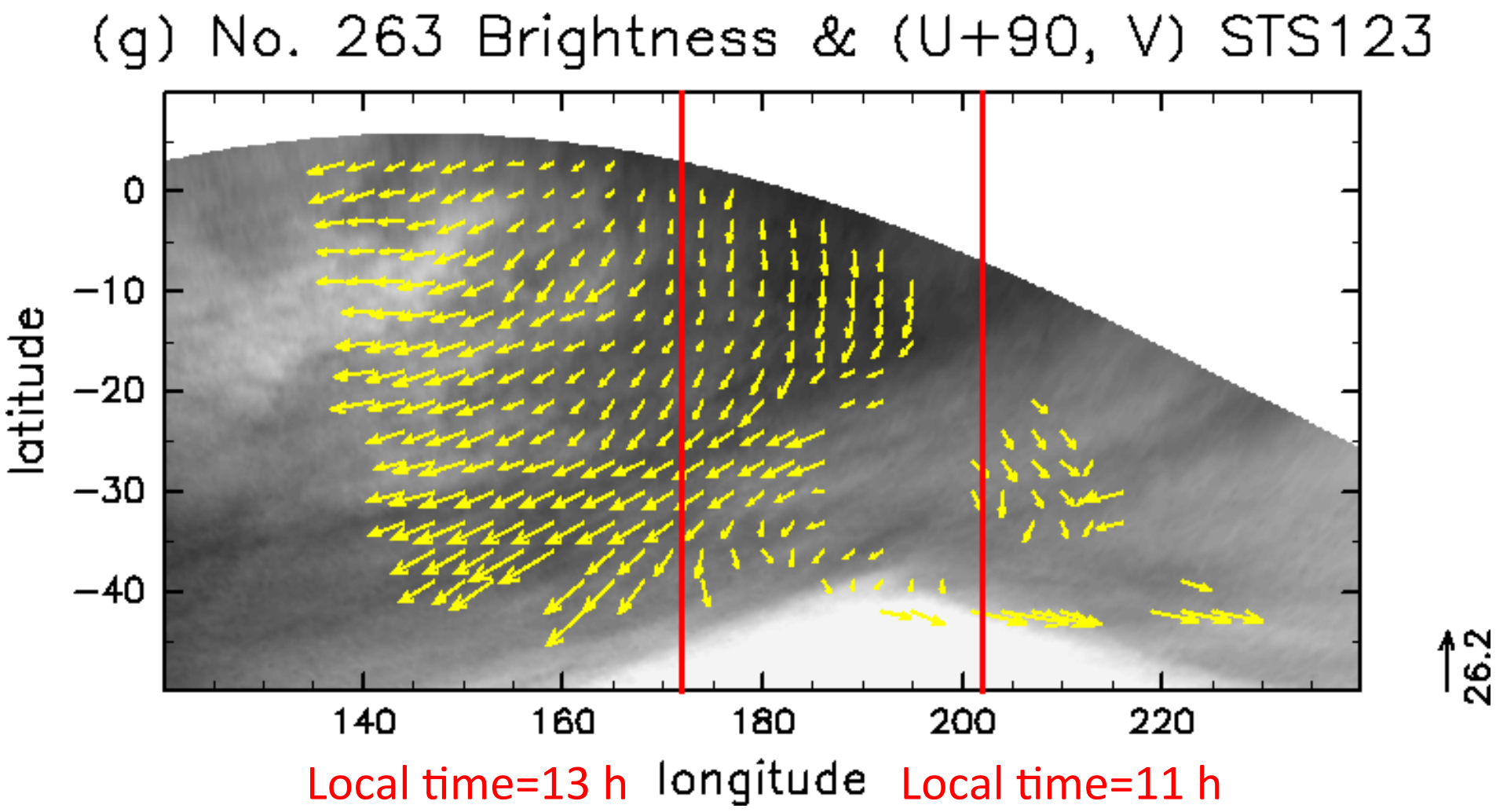
(g) No. 263 Brightness & (U+90, V) STS123
0
−10
−20
−30
−40
latitude
140
160
180
200
220
Local time=13 h
longitude
Local time=11 h
26.2

風速の水平分布（#265）

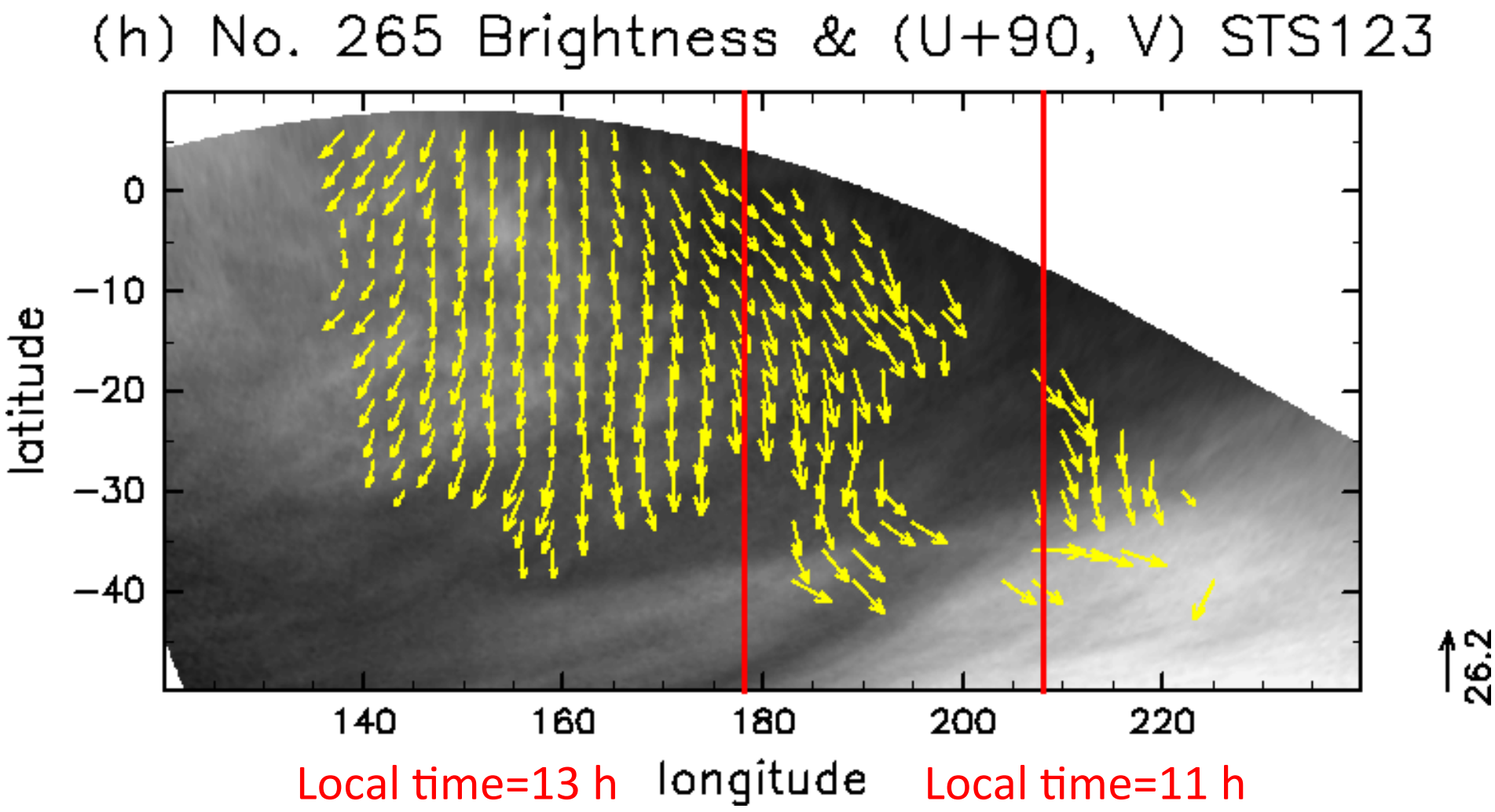
(h) No. 265 Brightness & (U+90, V) STS123
0
−10
−20
−30
−40
latitude
140
160
180
200
220
longitude
Local time=13 h
Local time=11 h
26.2

風速の水平分布（#266）

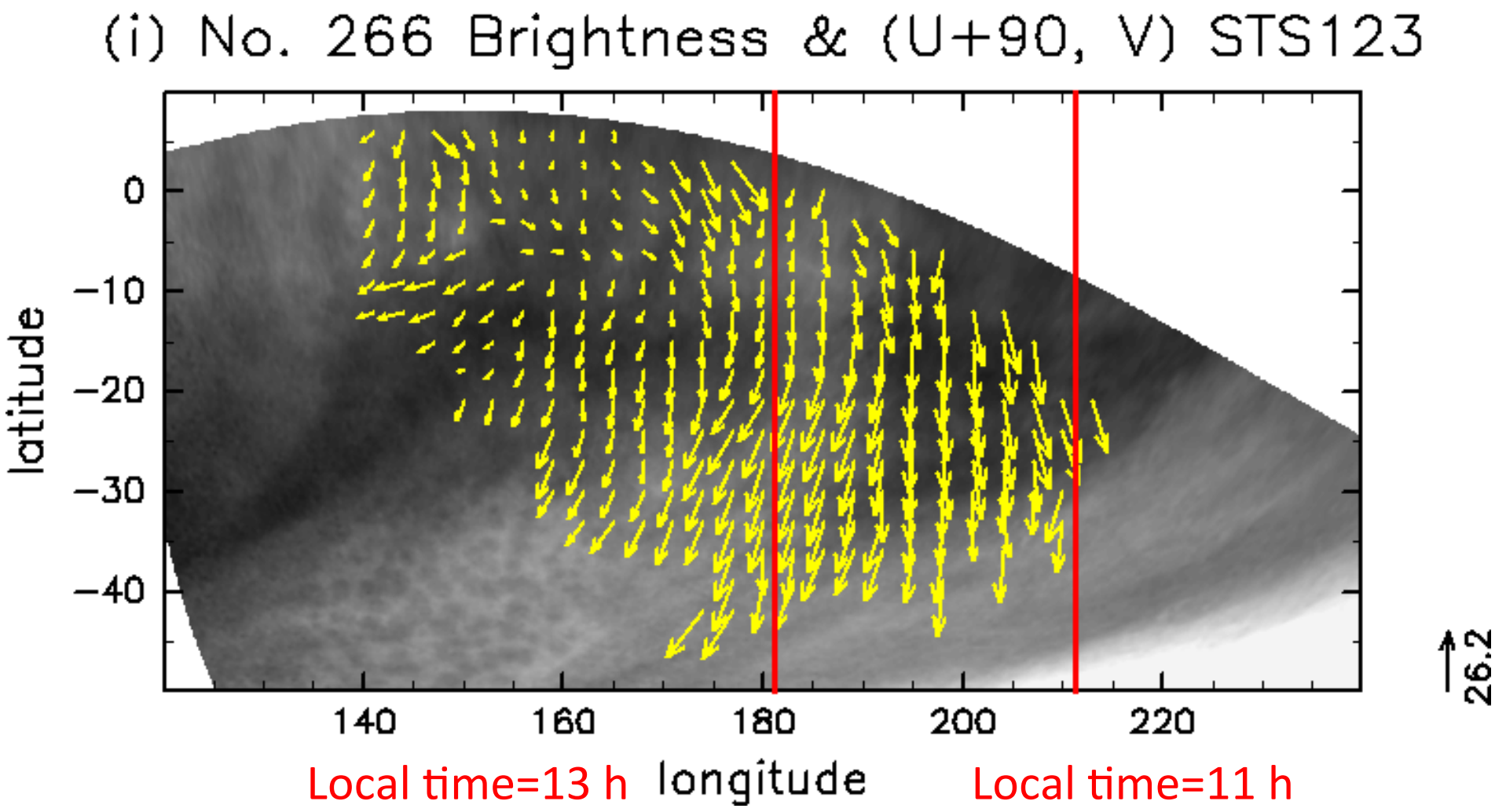
(i) No. 266 Brightness & (U+90, V) STS123
0
−10
−20
−30
−40
latitude
140
160
180
200
220
longitude
Local time=13 h
Local time=11 h
26.2

風速の水平分布（#267）

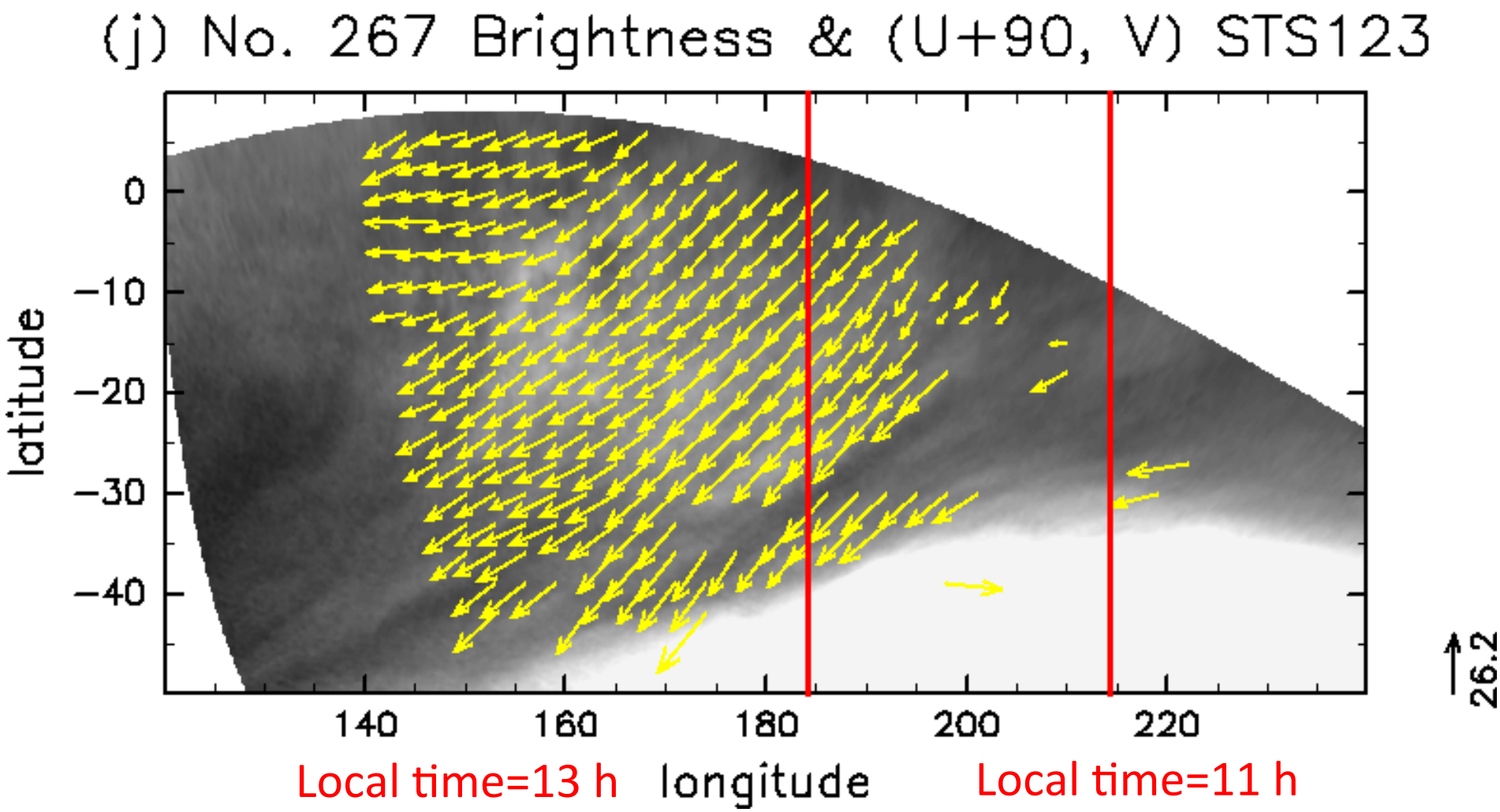
(j) No. 267 Brightness & (U+90, V) STS123
0
−10
−20
−30
−40
latitude
140
160
180
200
220
Local time=13 h
longitude
Local time=11 h
26.2

Comparison with earlier studies (mean zonal wind)

Note: longitudinal coverage in these studies are unknown → comparison limited

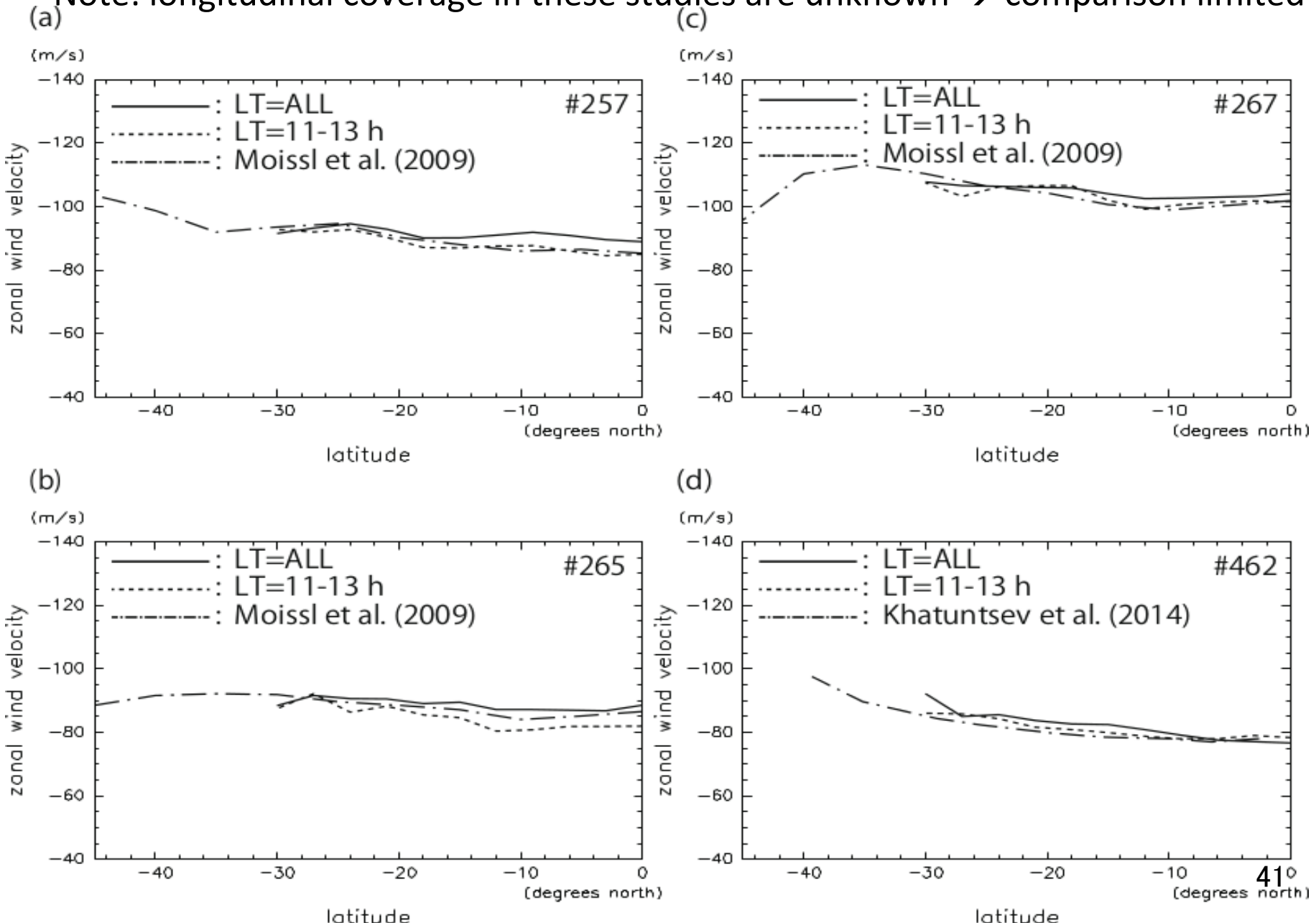

Time sequence of zonal winds (avg: 20S-EQ,LT11-13h)

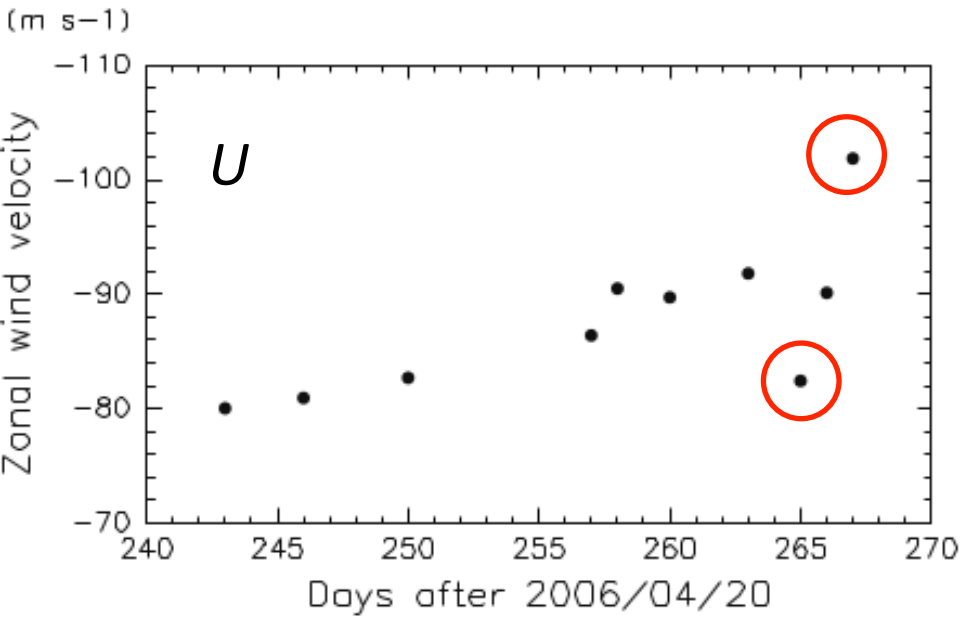

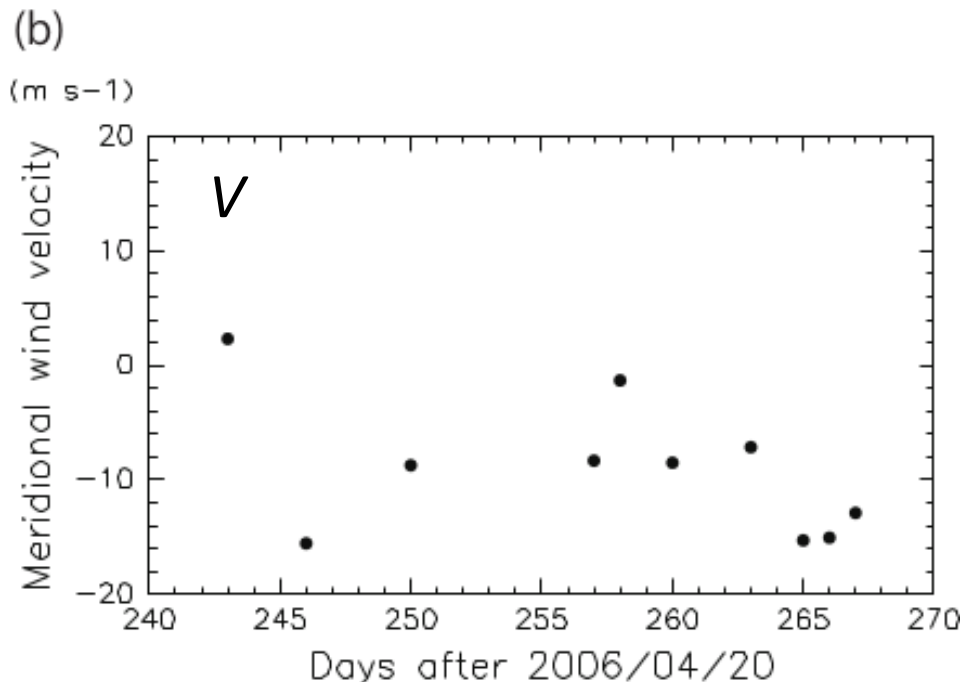

- Exists day-by-day fluctuation
  - No obvious periodicity → unable to explain by a single planetary-scale wave
  - U, V fluctuations: similar magnitude
  - ○ : Confirms the rapid intensification pointed out by Moissl et al (2009)

Tidal components (time average as func of LT&lat)

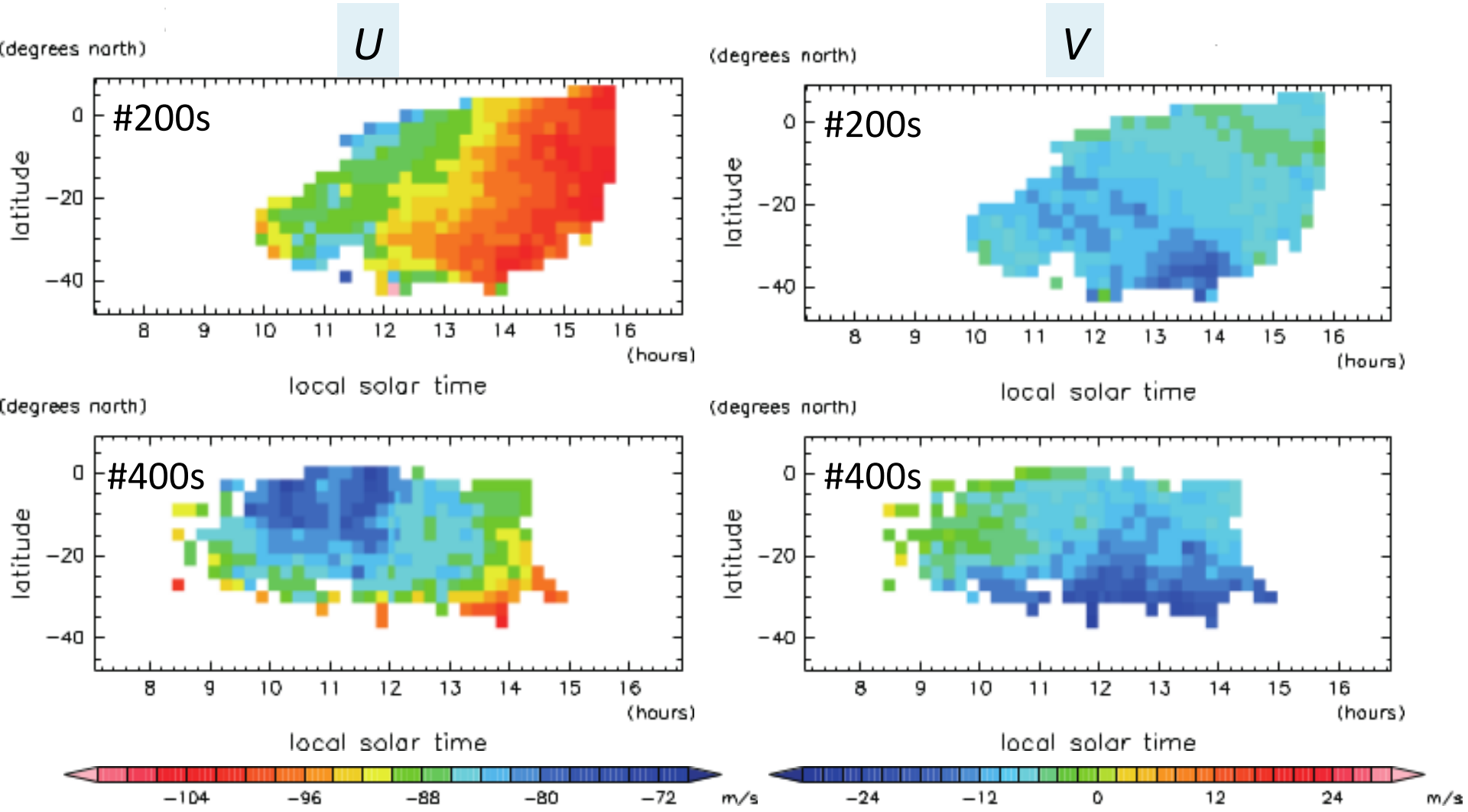

- Mean zonal wind : Period 2 (200s) > Period 3 (400s)
- Roughly speaking, consistent with Moissl et al. (2009) (period similar but only U is shown) and Khatuntsev et al. (2013) (U & V but the period is different)

What features are we really tracking?

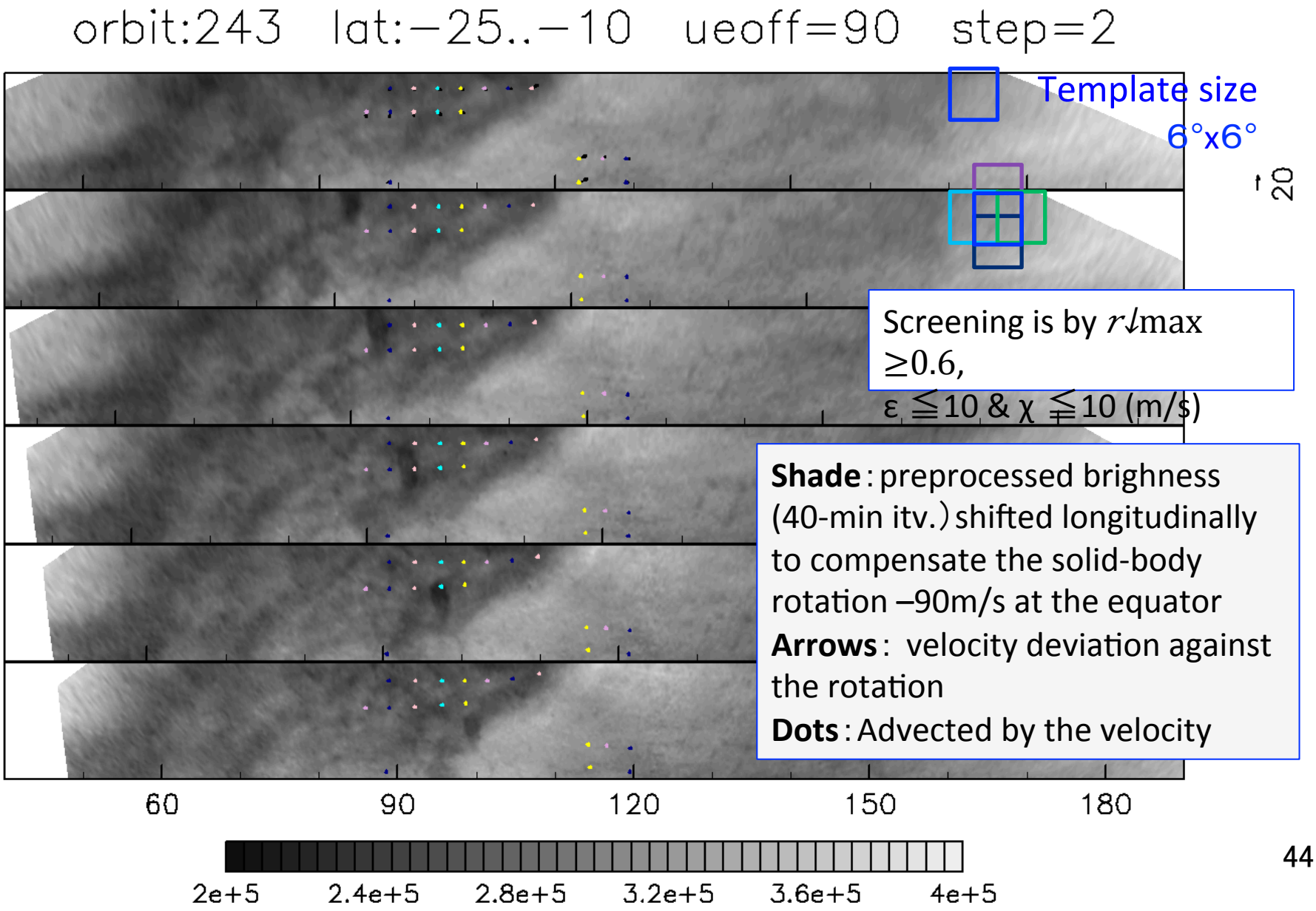

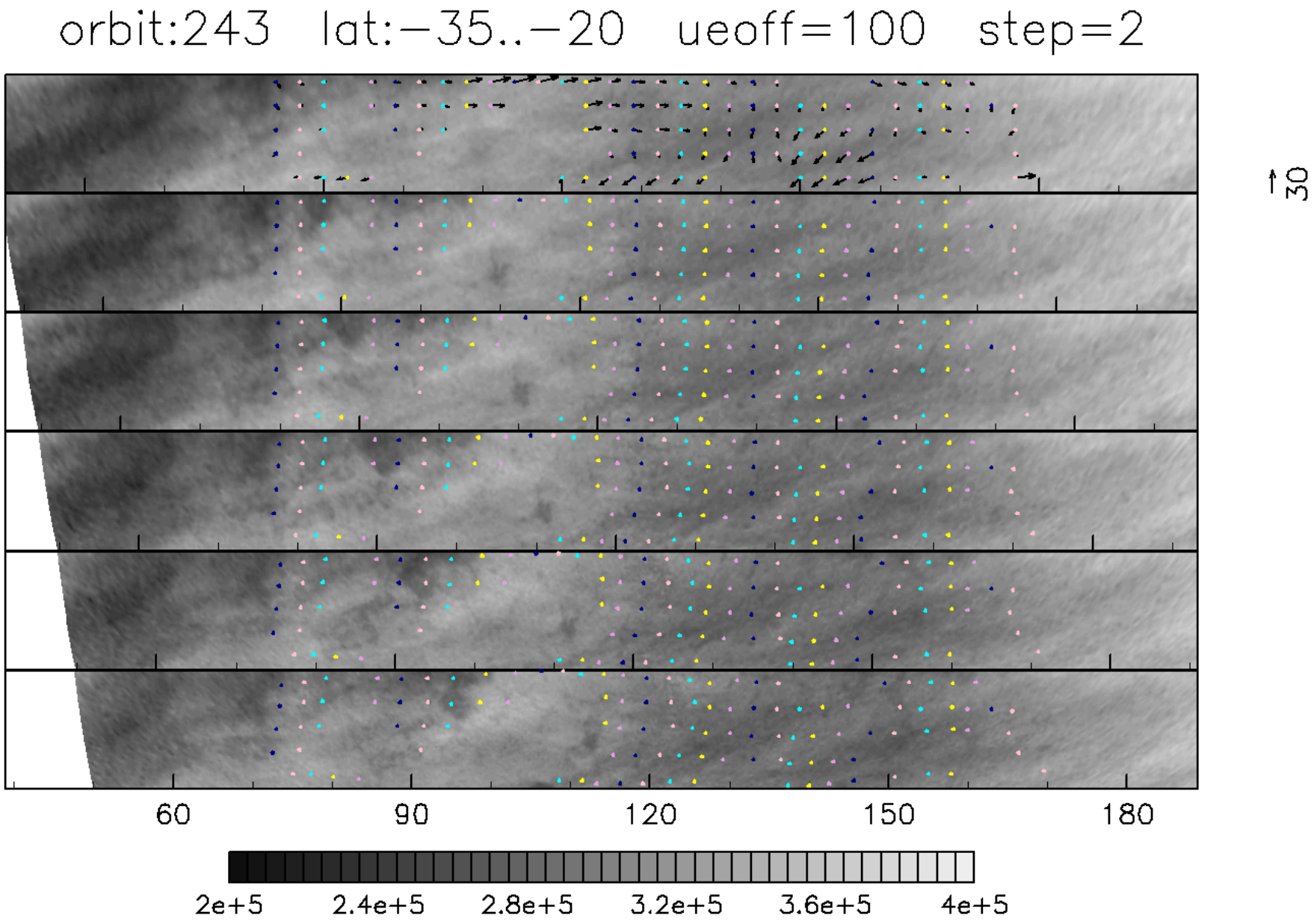
orbit:243 lat:−35..−20 ueoff=100 step=2
30
60
90
120
150
180
2e+5
2.4e+5
2.8e+5
3.2e+5
3.6e+5
4e+5

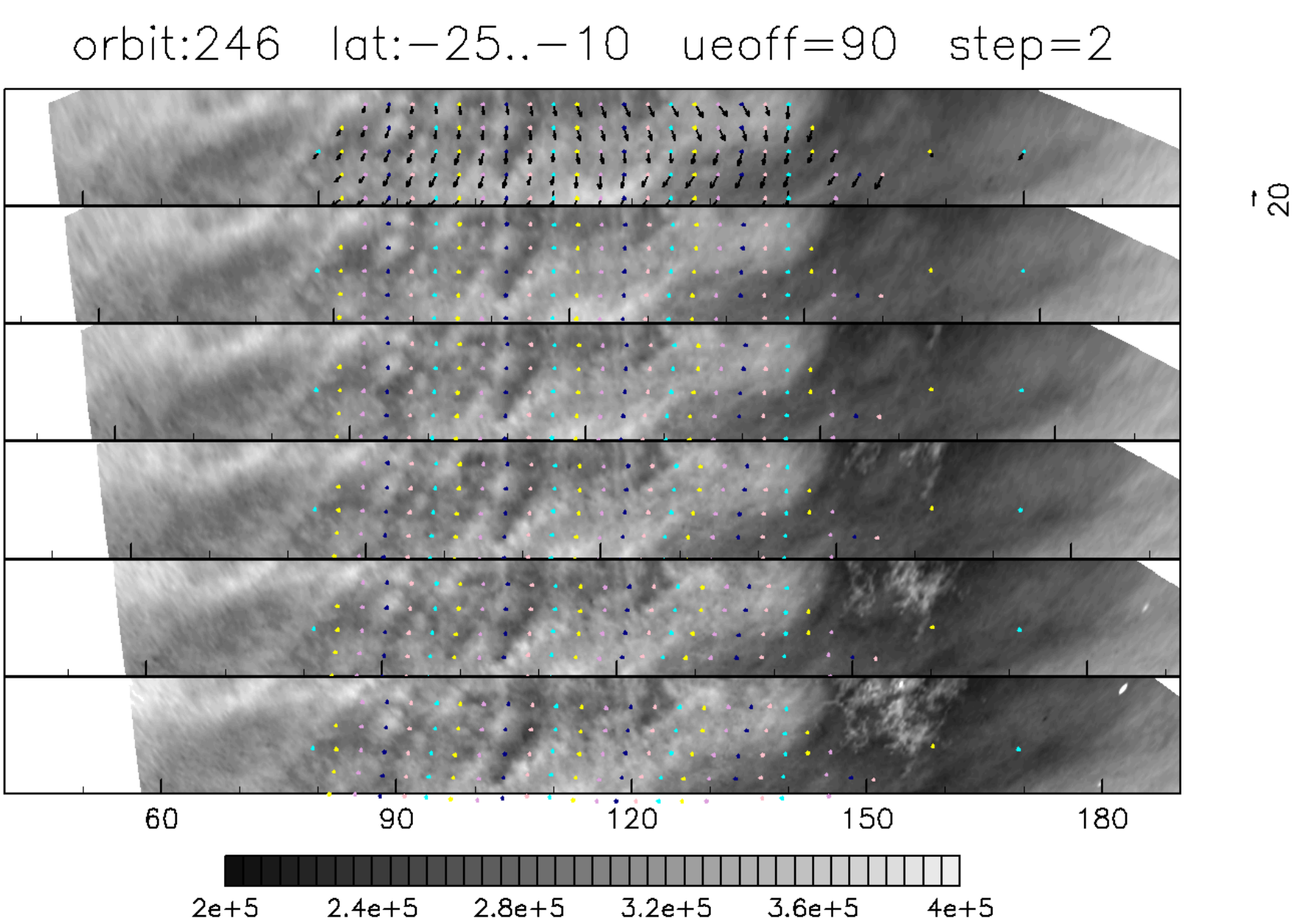
orbit:246 lat:−25..−10 ueoff=90 step=2
20
60
90
120
150
180
2e+5
2.4e+5
2.8e+5
3.2e+5
3.6e+5
4e+5

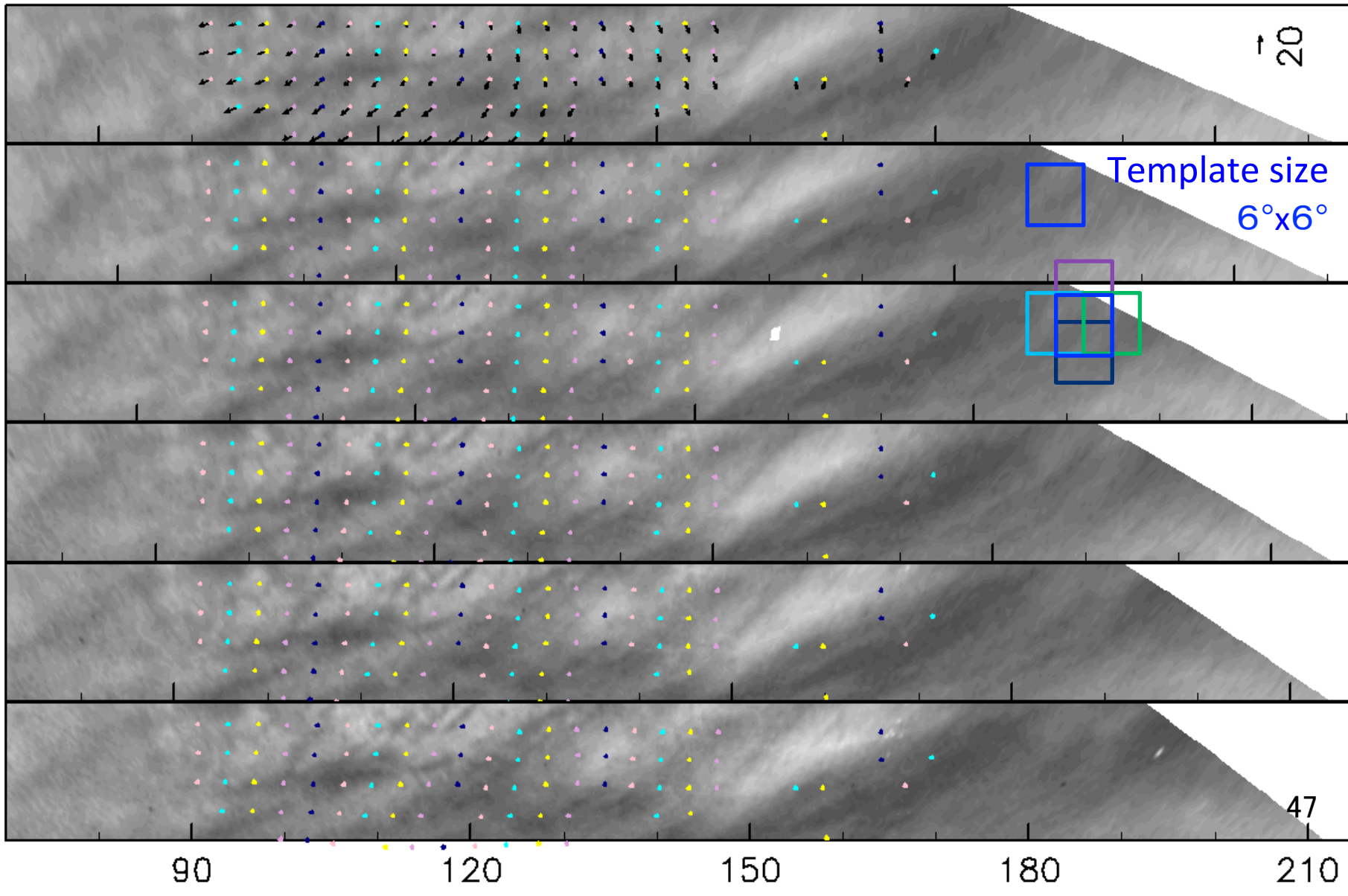
orbit:250 lat:−25..−10 ueoff=90 step=2
t 20
Template size
6°x6°
47
90
120
150
180
210

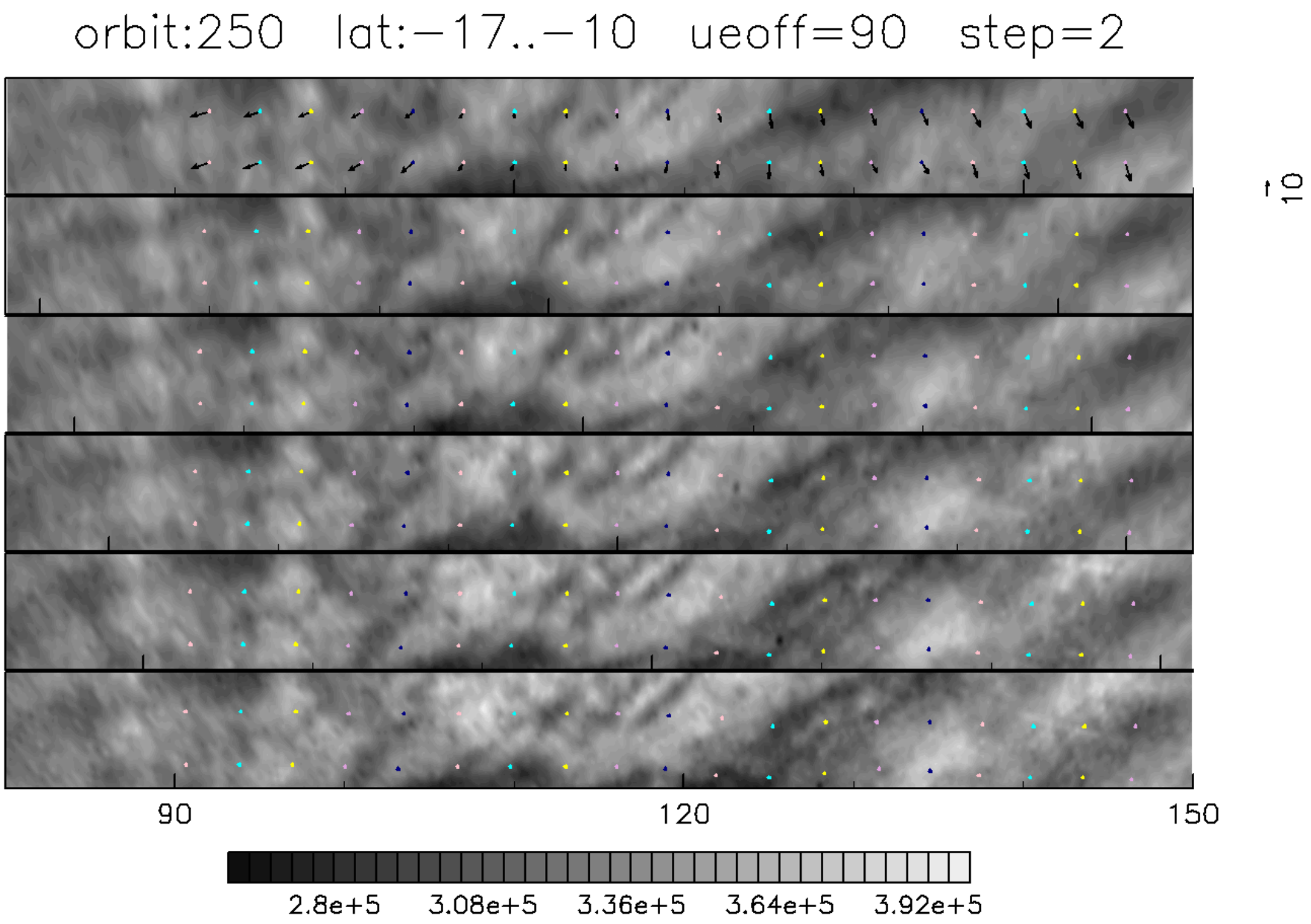
orbit:250 lat:−17..−10 ueoff=90 step=2
−10
90
120
150
2.8e+5
3.08e+5
3.36e+5
3.64e+5
3.92e+5

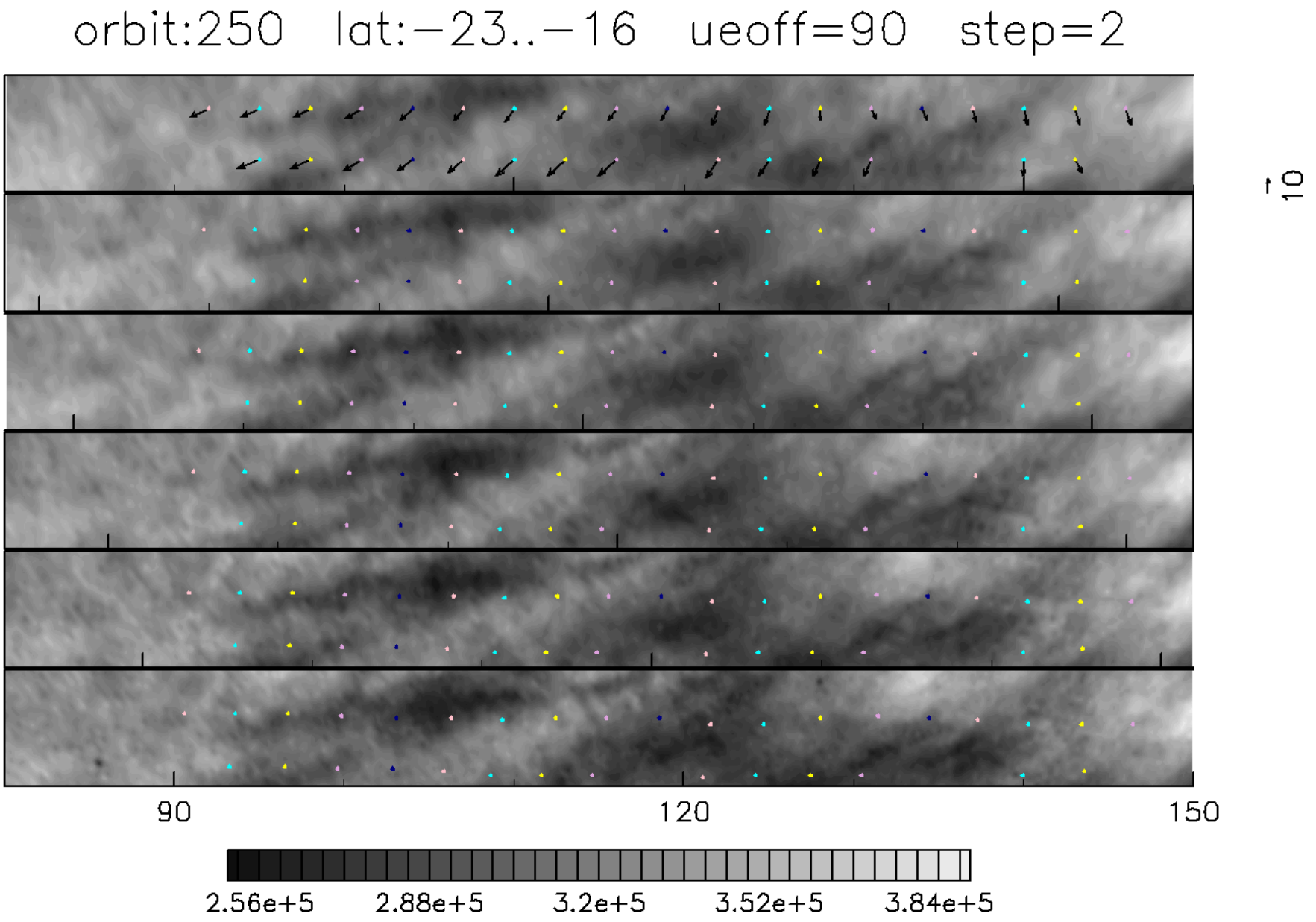
orbit:250 lat:−23..−16 ueoff=90 step=2
10
90
120
150
2.56e+5
2.88e+5
3.2e+5
3.52e+5
3.84e+5

Summary, Problems, Future outlook

- Superposition of CC surfaces improves the cloud tracking (increases the accuracy; suppresses erroneous match).
- Developed methods to evaluate the accuracy of **each** vector.
  - Mapped CC lower bound (ε) and error from 2-group comparison (χ). Can be used together for screening.
  - Results of VEX 200s → Typical value of χ is 2 m/s. Typical ε value is 8 m/s at low latitude & much greater at mid latitude.
  - Epoch making, **if** the error is as small as χ → enables one to study atmospheric disturbances (ang.-mom. flux, turbulence, instability…).
- Is this really so? (χ does not detect some errors: manual inspection suggests that error is sometimes much greater than χ. *Also, there is the lingering problem of CMV vs atmospheric wind at constant height*...)
- Improve the algorithm (Vary the template size and select according to ε and χ. Alternative peak selection as done by Koyama. Iteration. Affine transformation. Combine with a variational method...).
- Further development of error estimation

supplementary slides
(from IH15)

Effect of the spatial superposition (~running mean) of CC surfaces

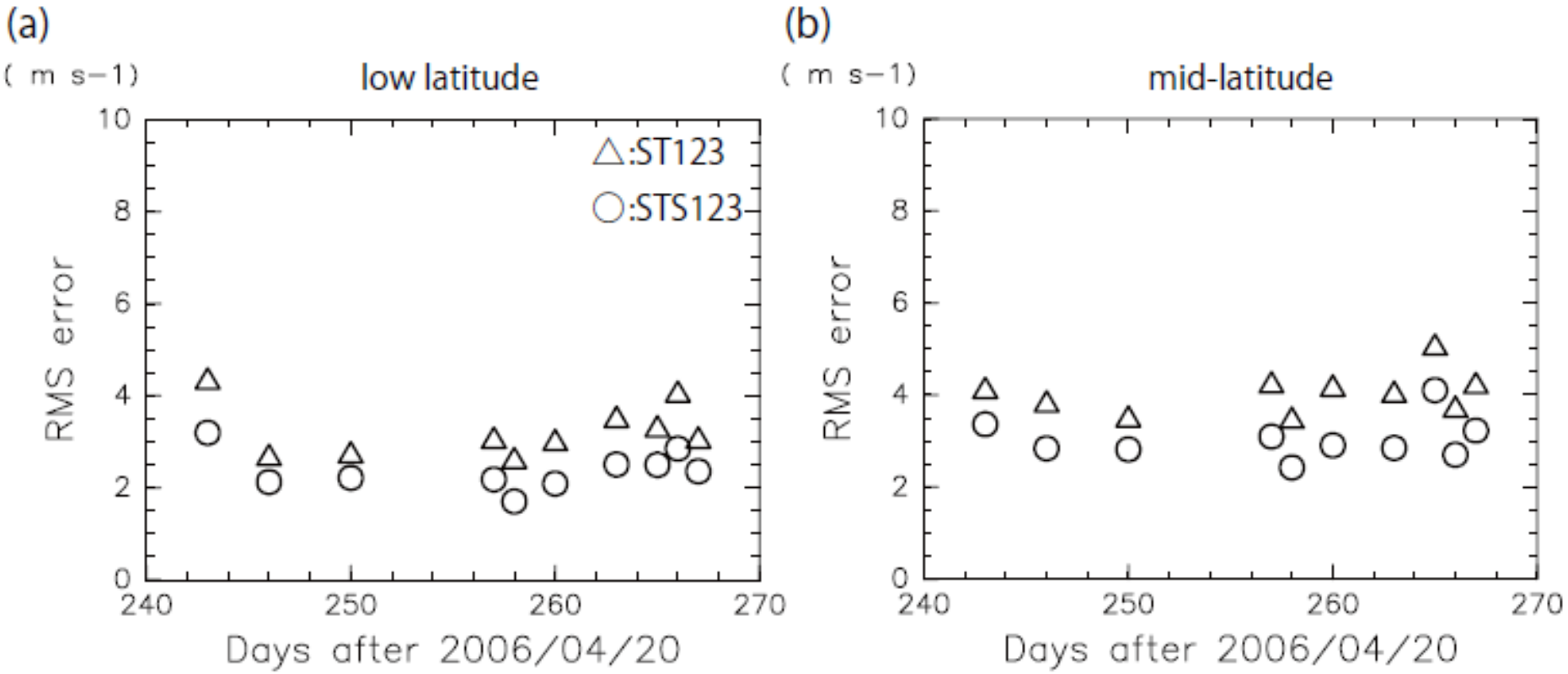

Effect of the distortion correction & limb fitting

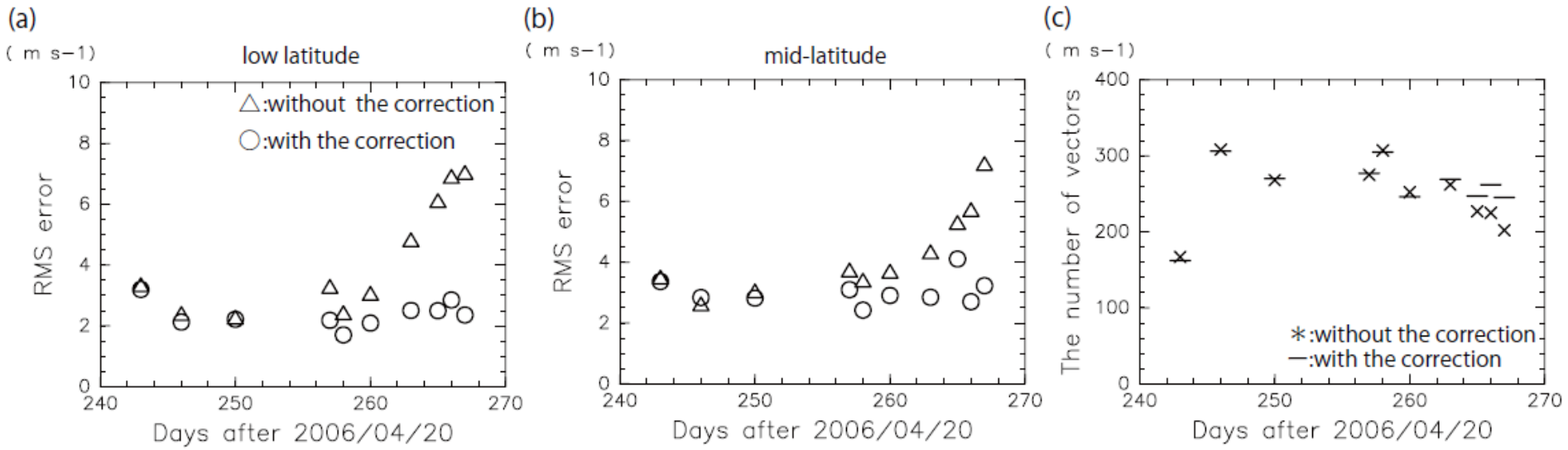

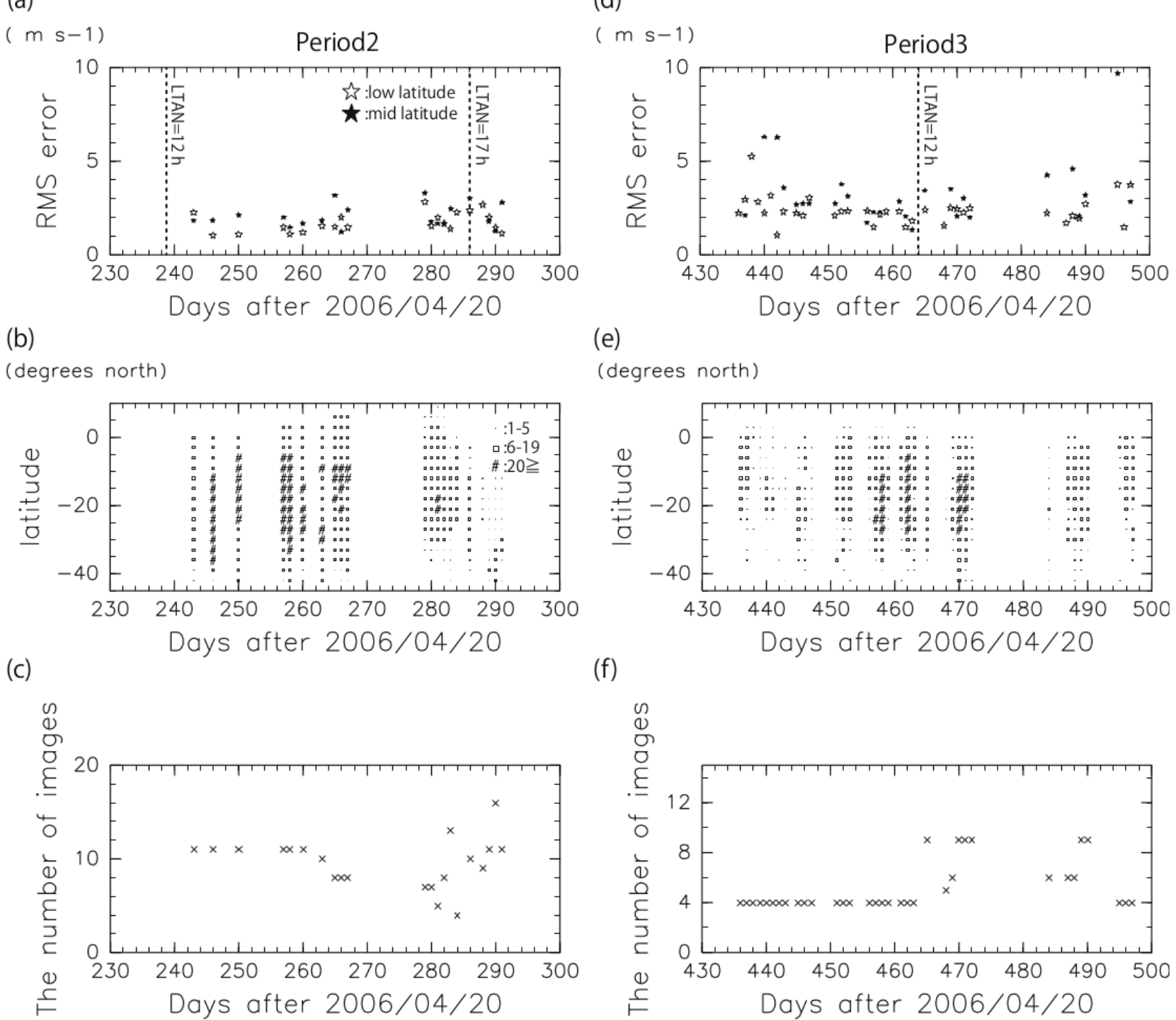
(a)
(m s−1)
Period2
RMS error
☆ :low latitude
★ :mid latitude
LTAN=12 h
LTAN=17 h
Days after 2006/04/20
(d)
(m s−1)
Period3
RMS error
LTAN=12 h
Days after 2006/04/20
(b)
(degrees north)
latitude
:1-5
□ :6-19
:20≦
Days after 2006/04/20
(e)
(degrees north)
latitude
Days after 2006/04/20
(c)
The number of images
Days after 2006/04/20
(f)
The number of images
Days after 2006/04/20

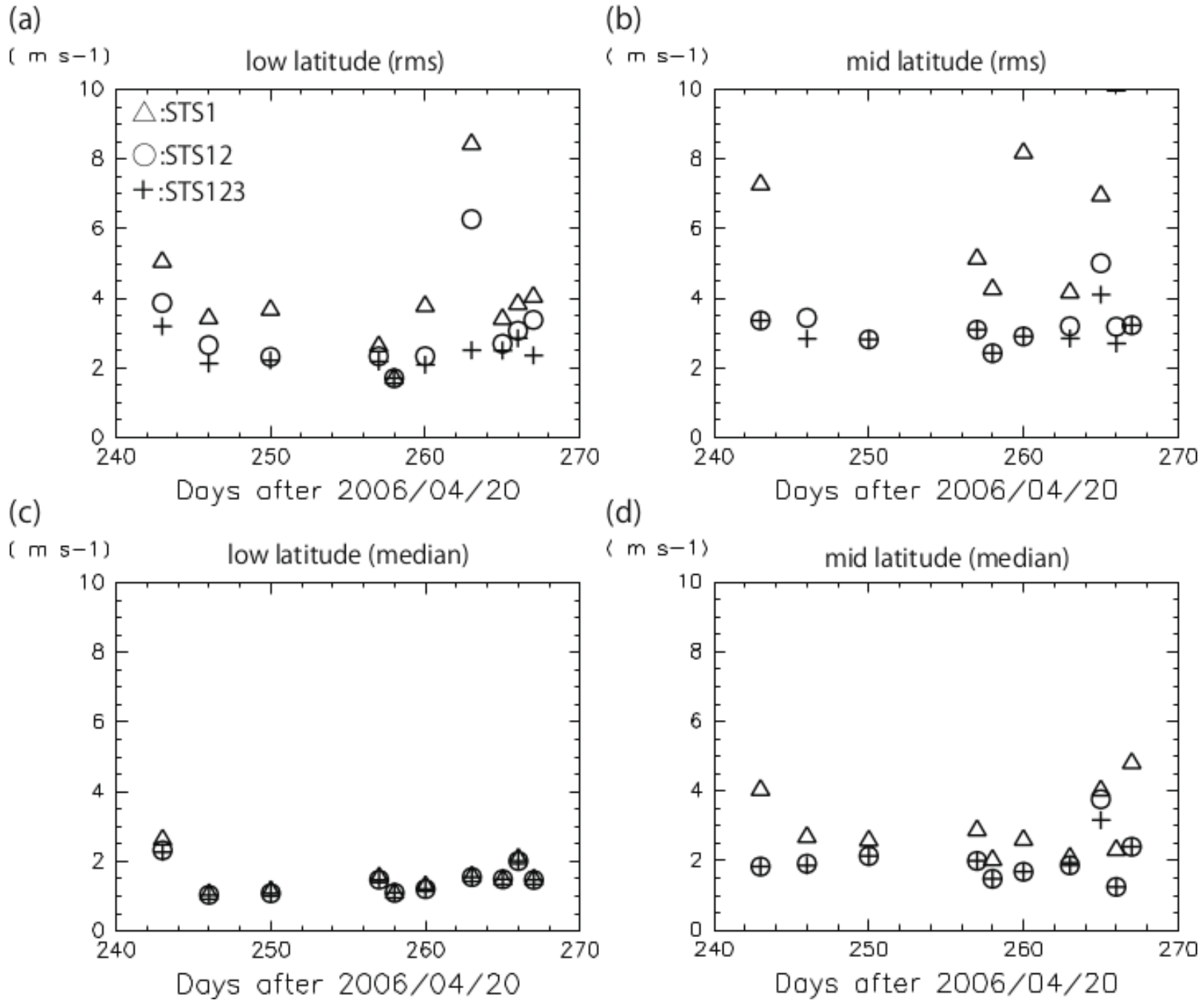
(a)
(m s−1)
low latitude (rms)
△:STS1
○:STS12
+:STS123
Days after 2006/04/20
(b)
(m s−1)
mid latitude (rms)
Days after 2006/04/20
(c)
(m s−1)
low latitude (median)
Days after 2006/04/20
(d)
(m s−1)
mid latitude (median)
Days after 2006/04/20

$$r(\lambda_a, \phi_b, u_{\hat{l},b}, v_{\hat{m}}) = \frac{1}{P}\sum_{p=1}^{P} r_p(\lambda_a, \phi_b, u_{\hat{l},b}, v_{\hat{m}}). \tag{15}$$

$$r_p(\lambda_a, \phi_b, u_{\hat{l},b}, v_{\hat{m}}) \equiv r^{n,n+k}(\lambda_a, \phi_b, u_{\hat{l},b}, v_{\hat{m}}). \tag{13}$$

$p = 1, 2, \cdots, P$ to represent the combinations of t_n and t_{n+k}

$$r^{n,n+k}(\lambda_a, \phi_b, u_{l,b}^{n,n+k}, v_m^{n,n+k}) \equiv r_{a+\Delta a,b+\Delta b,l,m}^{n,n+k}, \tag{8}$$

$$\Delta a \equiv \text{round}\left[\frac{u_{l,b}^{n,n+k}(t_n - t_0)}{\Delta\lambda R_c \cos\phi_b}\right], \quad \Delta b \equiv \text{round}\left[\frac{v_m^{n,n+k}(t_n - t_0)}{\Delta\phi R_c}\right]. \tag{9}$$

$$u_{l,b}^{n,n+k} = \frac{l\Delta\lambda R_c \cos\phi_b}{t_{n+k} - t_n}, \tag{6}$$

$$v_m^{n,n+k} = \frac{m\Delta\phi R_c}{t_{n+k} - t_n}, \tag{7}$$

$$r_{a,b,l,m}^{n,n+k} = \frac{\sum_{i=-\frac{I}{2}}^{\frac{I}{2}-1}\sum_{j=-\frac{J}{2}}^{\frac{J}{2}-1}(F_{a+i,b+j,n} - \bar{F}_{a,b,n})(F_{a+l+i,b+m+j,n+k} - \bar{F}_{a+l+i,b+m+j,n+k})}{\sqrt{\sum_{i=-\frac{I}{2}}^{\frac{I}{2}-1}\sum_{j=-\frac{J}{2}}^{\frac{J}{2}-1}(F_{a+i,b+j,n} - \bar{F}_{a,b,n})^2}\sqrt{\sum_{i=-\frac{I}{2}}^{\frac{I}{2}-1}\sum_{j=-\frac{J}{2}}^{\frac{J}{2}-1}(F_{a+l+i,b+m+j,n+k} - \bar{F}_{a+l+i,b+m+j,n+k})^2}}, \tag{4}$$

$$\bar{F}_{a,b,n} \equiv \frac{1}{IJ}\sum_{i=-\frac{I}{2}}^{\frac{I}{2}-1}\sum_{j=-\frac{J}{2}}^{\frac{J}{2}-1} F_{a+i,b+j,n}. \tag{5}$$

Appendix A. Estimation of the effective degrees of freedom

The effective degrees of freedom of the superposed cross-correlation is for formulated in this section. The effective degrees of freedom of a simple cross-correlation, which is used in the tracking based on a single image pair, can be expressed by a standard formula (e,g, Thomson and Emery, 1994) as

$$M_e^{(1)} = \frac{M}{\Omega^{(1)}}, \tag{A.1}$$

$$\Omega^{(1)} = \sum_{\tau=-M}^{M} \left(1 - \frac{|\tau|}{M}\right) R_{xx}^{(1)}(\tau) R_{yy}^{(1)}(\tau), \tag{A.2}$$

where τ is the lag, M is the number of pixels, and $R_{xx}^{(1)}$ and $R_{yy}^{(1)}$ are the auto correlations:

$$R_{xx}^{(1)}(\tau) = \frac{M}{M-\tau} \frac{\sum_{\omega=1}^{M-\tau} x'(\omega) x'(\omega+\tau)}{\sum_{\omega=1}^{M} x'(\omega)^2}, \tag{A.3}$$

$$R_{yy}^{(1)}(\tau) = \frac{M}{M-\tau} \frac{\sum_{\omega=1}^{M-\tau} y'(\omega) y'(\omega+\tau)}{\sum_{\omega=1}^{M} y'(\omega)^2}, \tag{A.4}$$

where dash represents the deviation from the sample mean. In our problem, x and y are one-dimensionalized brightness sequences from sub-regions, so $M = IJ = 48^2 = 2304$. Note that the way how the two-dimensional sub-image data is one-dimensionalized does not affect $\Omega^{(1)}$, since Eq. (A.2) can be rewritten as

$$\Omega^{(1)} = \frac{\frac{1}{M}\sum_{t=1}^{M}\sum_{s=1}^{M} x(t)x(s)y(t)y(s)}{\sqrt{\frac{1}{M}\sum_{t=1}^{M}\{x(t)\}^2}\sqrt{\frac{1}{M}\sum_{t=1}^{M}\{y(t)\}^2}}. \tag{A.5}$$

The effective degree of freedom is evaluated for the combination of the template and target regions that maximize the cross-correlation. Thus, $R^{(1)}_{xx}$ and $R^{(1)}_{yy}$ generally have similar values. Eq. (A.2) is suitable to estimate $\Omega^{(1)}$ when x and y have a high correlation.

We define the effective degree of freedom for the superposed cross-correlation defined by Eq. (15) can be estimated as

$$M_e \equiv \frac{PM}{\Omega}, \tag{A.6}$$

$$\Omega \equiv \frac{1}{P}\sum_{p=1}^{P}\Omega^{(p)}, \tag{A.7}$$

where $\Omega^{(p)}$ is the correlation length obtained from the p-th pair of images by using Eq. (A.2). Eqs. (A.6) and (A.7) are justified

by using Eqs. (A.1) and (A.2) as follows. The superposed cross-correlation r of Eq. (15) can be rewritten as

$$r = \frac{1}{p}\sum_{p=1}^{P} r_p = \frac{1}{P}\sum_{p=1}^{P} \frac{\mathrm{Cov}(x^{(p)}, y^{(p)})}{\sigma_{x^{(p)}}\sigma_{y^{(p)}}}, \tag{A.8}$$

where Cov and σ represent covariance and standard deviation, and $x^{(p)}$ and $y^{(p)}$ represent the brightness sequence of template and target subimages of the p-th pair. If $\sigma_{x^{(p)}}$ and $\sigma_{y^{(p)}}$ can be approximated by a common constant σ (Approximation A), the r of Eq. (A.8) is approximated as

$$r \simeq \frac{1}{\sigma^2 P}\sum_{p=1}^{P} \mathrm{Cov}(x^{(p)}, y^{(p)}) = \frac{1}{\sigma^2}\frac{1}{PM}\sum_{t=1}^{PM} X_t Y_t, \tag{A.9}$$

where X_t and Y_t $(t = 1, 2, \cdots, PM)$ represent concatenated brightness sequences over the P pairs. In this case, the correlation length is written as

$$\Omega_c \equiv \sum_{\tau=-PM}^{PM} \left(1 - \frac{|\tau|}{PM}\right) R_{xx}^{(1)}(\tau) R_{yy}^{(1)}(\tau), \tag{A.10}$$

from Eq. (A.2), and the effective degree of freedom is expressed as $\frac{PM}{\Omega_c}$, since the data length is PM. Since Approximation A is expected to be valid, Ω and Ω_c are expected to have similar values. Therefore, Eqs. (A.6) and (A.7) are, which justifies Eqs. (A.6) and (A.7).